FACULDADE DE ENGENHARIA DA UNIVERSIDADE DO PORTO

Omnidirectional GPS Antenna For Vorsat

João Pedro Lisboa Pinto

Mestrado Integrado em Engenharia Electrotécnica e de Computadores

Supervisor: Sérgio Reis Cunha (Prof.Doutor)

September 2011

Omnidirectional GPS Antenna For Vorsat

João Pedro Lisboa Pinto

Mestrado Integrado em Engenharia Electrotécnica e de Computadores

Aprovado em provas públicas pelo Júri:

Presidente: Artur Andrade Moura (Prof.Doutor)

_____

Arguente: Paulo Mateus Mendes (Prof.Doutor)

_____

Vogal: Sérgio Reis Cunha (Prof.Doutor)

_____

28 de Setembro de 2011

Resumo

O desenvolvimento de satélites de reduzidas dimensões e peso, geralmente denominados por CubeSats, é uma área que tem sido alvo de atenção nos últimos anos. Com efeito, estes têm sido lançados em particular para uma LEO, com o propósito não só de estudar determinados parâmetros do seu comportamento em órbita, como também para testar determinados aspectos da comunicação em órbita, características da sua reentrada na Terra, ou de transportar experiências biológicas a ser conduzidas a baixa gravidade. Esta dissertação surge então da necessidade de um CubeSat denominado Vorsat, de conhecer a sua posição espacial por GPS em qualquer instante. Para tal, é necessária a existência de uma antena receptora GPS que o possibilite. Devido às características inerentes ao próprio funcionamento do GPS, e ao movimento incontrolado de constante rotação do satélite, impõe-se assim a utilização de uma antena cujo Diagrama de Radiação que aproxime a Isotropia. Posto isto, esta Dissertação aborda precisamente a implementação de um "array" de Polarização Circular de "Trimmed Square Microstrip Patch Antennas" para a criação do Padrão referido. Para o efeito, dois programas orientados para o "design" são realizados. Um primeiro em que um método que utiliza o Modelo de Transmissão para Linhas Microstrip, e cortes na "Patch" para criar Polarização Circular, é utilizado para projectar as sub antenas do "array". Um outro de simulação, para a determinação das características do "array". Um protótipo deste "array" de antenas é criado e testes e conclusões são apresentados.

ii

Abstract

The development of satellites with low dimensions and weight, usually named CubeSats, is an area that has been paid attention in recent years. This kind of satellites, has been launched particularly to a LEO. Its purpose is usually, to study certain parameters of its orbit behaviour, to test some aspects of in orbit communication, to study the characteristics of its Earth re-entry and also, for example, to transport biological experiments in low gravity. It's from the need of a CubeSat named Vorsat to know its spatial position at any moment, using GPS, that this thesis gets its purpose. For such application a GPS receiver antenna is needed. Due to the characteristics inherent to the GPS operation, and also due to the constant uncontrolled rotational movement of the satellite, an antenna with a Radiation Pattern that approximates Isotropy becomes essential. That said, this thesis addresses precisely the implementation of a Circular Polarized Trimmed Corners Square Microstrip Patch Antenna array with a near Isotropic Pattern. To do so, two software were developed. The first one is related to the design of the sub antennas that constitute the array. Although it's widely based on the Transmission Line Model, it also uses the Truncated Corner Method to implement Circular Polarization. The other software is a simulation one and it's used to determine the characteristics of the array of antennas itself. A prototype of this antenna array is built and the tests and conclusions drawn out are presented.

Acknowledgements

First, I would like to thank my supervisor, Professor Sérgio Reis Cunha, for all the support that he gave me during this last couple of months. Without this support it wouldn't be possible to finish this thesis. I would also like to thank my family, particularly my sisters and my parents for all the the opportunities and love that they gave me throughout all my life. To my friends and colleagues , I thank you for all the support and companionship during this five years. In particular I thank the help provided by my colleagues Filipe Monteiro and Ricardo Pinto during this last months of course conclusion. To all the above mentioned and also to those that in some way made a contribute for this thesis, I express my sincere thank you.

João Pedro Lisboa Pinto

"A good head and a good heart
are always a formidable combination"

Nelson Mandela

Contents

List of Figures

List of Tables

Abbreviations and Symbols

CAD   Computer-Aided Design
GNSS   Global Navigation Satellite Systems
GPS   Global Positioning System
LEO   Low Earth Orbit
FEUP   Faculty of Engineering of the University of Porto
PCB   Printed Circuit Board

Chapter 1

Introduction

This chapter serves as an introduction to the scope of this thesis, which documents the final project of the MSc in Electric and Computer Engineering at the University of Porto. It's intended for the reader to generically understand the main themes that are further developed and to have an idea of the main steps involved in this development. To this end, this chapter is divided into: "Motivation", "Objectives and Work plan" and "Thesis Structure".

1.1 Motivation

Since there are records of Humankind's existence, it has been found that humans have an imperative need to communicate. This necessity led to the invention of long distance communication. Initially primitive methods were developed, e.g., Smoke Signals and Audio Signals. However telecommunications as known today were only made possible in 1873. This was the year when the Theories of Electricity and Magnetism were finally unified, through what later became known as "Maxwell's Equations". However it took until 1901 for the first Transatlantic Messaging system to be created, by Marconi.

The next big leap in telecommunications occurred in Second World War. During this period a lot of efforts were put into the development of Antenna Theory and into the Computational field. By combining these two sciences several new antenna designs were developed. From then on this new field's progress has been fast paced [22],[23]. So much so that nowadays most telecommunication control has left its terrestrial roots and is now mostly done from space.

This thesis main goal is to develop an antenna with certain properties, so that it can be incorporated into a broader project named Vorsat. The latter's objective is to design and build a LEO satellite. It's from the need that this satellite has, when in orbit, to be fed its

GPS location, its velocity and the current time with a certain level of accuracy that makes it essential to have a proper GPS antenna as part of the Telecommunication System. But the antenna here proposed would also have to fulfil the requirements of the mentioned project. Quoting [22] " For wireless communication systems, the antenna is one of the most critical components. A good design of the antenna can relax system requirements and improve overall system performance. A typical example is TV for which the overall broadcast reception can be improved by utilizing a high performance antenna ". The same author also emphasizes the importance of the Directional property of the antenna, on any wireless system, as a means of improving its overall performance. This same property arises as one of the fundamental requirements of the antenna here developed and it's also a main topic throughout this thesis. It's known that the satellite in question will be in constant rotation on different axes, and its orientation at each instant will be unknown. This implies that for it to be able to receive GPS signals continuously, it's necessary for the antenna Radiation Pattern to be ideally Isotropic. However, taking into account that theoretically this pattern isn't feasible, the objective is then to create one that approximates isotropy. With this in mind, given the cubic structure of the satellite, there are six faces where one can place the antenna in order to obtain the desired pattern. Given this spatial configuration, the solution that will be researched for this problem assumes the form of an array of sub-antennas. There are yet some other requirements/constraints related either to GPS transmission or to the project itself. Examples of these are: the physical structure of the antenna, the Bandwidth, the Polarization, Radiation Efficiency and the Gain.

1.2   Objectives and Work plan

The main objectives of this thesis are as follows:

1   Define the structure of the sub-antennas to be placed in each face of the satellite. Determine its characteristics.

2   Design the antenna array so that the Radiation Pattern is as close to Isotropy as possible, not disregarding the need for Right Hand Circular Polarization. Utilize simulation tools.

3   Implement the previously defined sub-antennas.

4   Test and characterize the implemented array using the anechoic chamber.

With the main objectives of this thesis defined, the Work plan is next presented under the form of a Gantt Chart, visible in figure 1.1.

Tasks	February	March	April	May		June	July
	01-30	01-30	01-30	01-15	16-31	01-30	01-31
1. Study of Antenna's General Properties and Theory.							
2. Study and Development of Microstrip Patch Antennas to be used as Sub-Antennas of the Array.							
3. Study and Design of the Array.							
4. Implementation of the Array.							
5. Thesis Writing.							

Figure 1.1: Work plan

1.3 Thesis Structure

Besides the Introduction, this thesis has six more chapters. In chapter 2, some concepts considered necessary to the understanding of this Dissertation are stated. In chapter 3, the Literature Review is handled. In chapter 4, the design process of the sub antennas that constitute the antenna array is presented. Also the theory that is behind it is described. In chapter 5, the software built for the array designed is presented, as well as the results and conclusions drawn from it. In chapter 6, the implemented prototype of the antenna array is presented. Tests and results performed are respectively described and given. As result of this process some conclusions are made. In chapter 7, the conclusions of the whole thesis are stated as well as the future work.

Finally it should be pointed out that apart from this chapter, in the end of each main chapter, a brief summary is to be expected.

Chapter 2

Basic Antenna Concepts

In this chapter some concepts considered to be essential in order for the reader to have a better understanding of the themes discussed throughout this thesis are presented. These are all antenna parameters, used for its characterization . According to [2]an antenna can be defined as: " ... an antenna is a transition device, or transducer, between a guided wave and a free-space wave,or vice versa.". It's from the need for a better description of this conversion function that the following parameters become useful.

2.1   Radiation Pattern

The Radiation Pattern describes the radiation properties of an antenna as a function of spatial coordinates. In the creation of this diagram, properties like Power Flux Density, Radiation Intensity, Polarization or Field Strength(Electric or Magnetic) are used. These can be represented in either a mathematical or a graphical way. This diagram is often used in the Far-Field Region(defined for distances bigger than $\frac{2*D^2}{\lambda}$ in which D is the biggest overall dimension of the antenna and λ is the wavelength), in which the Radiation Pattern of the antenna is independent of the distance to the antenna. It is possible to categorize antennas into three distinctive groups, trough the analysis of its pattern, by classifying it as: Isotropic, Directional or Omnidirectional.

An Isotropic Radiation Pattern is recognized for radiating equally in all directions, i.e. independently of spatial coordinates.

On the other hand the Directional Radiation Pattern distinguishes itself by radiating in a more focused way. This means that a directional antenna receives/radiates electromagnetic waves in some directions better than on the others. Such pattern is generally defined as having a relatively bigger directivity than the half-wave dipole [1].

Finally, the Omnidirectional Radiation Pattern is characterized by the existence of a plane in which the radiation occurs in a non directional way and another one, orthogonal to the first one, in which the antenna radiates in a directional way.

In figure 2.1 it's possible to see some schemes regarding the Radiation Patterns that have been previously described.
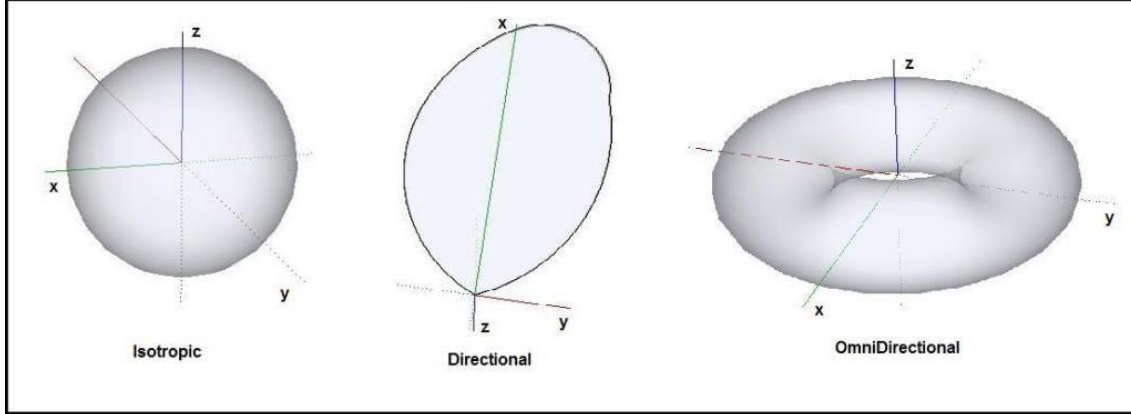
Figure 2.1: Radiation Patterns

2.2   Radiation Power Density

This parameter is closely related to the energy/power associated with the Electric and Magnetic Fields that constitute the Electromagnetic Waves radiated by an antenna. It uses in its definition the Poynting Vector, whose instantaneous definition is given as being the cross product between the instantaneous Electric and Magnetic Field. By integrating this over a closed surface(S), it is possible to obtain the Total Instantaneous Radiated Power. However, the most convenient and usually the most used definition is the Average Power Density, which is mathematically expressed according to equation 2.1. In this equation **E** and **H** are respectively the phasors of the Electric and Magnetic Fields.

$$Prad = \frac{1}{2} \oint_S Re(\mathbf{E} \times \mathbf{H}^*) \cdot ds \tag{2.1}$$

2.3   Radiation Intensity

The Radiation Intensity U is mathematically expressed by $\frac{r^2}{2} \oint_S Re(\mathbf{E} \times \mathbf{H}^*) \cdot ds$, in which r is the distance between the spatial point in which this is being measured. According to [1], this intensity can be defined as the power radiated by an antenna per solid angle unity, for a given direction. The SI units of solid angle are named steradian. For a better understanding of this measure, figure 2.2 is presented.
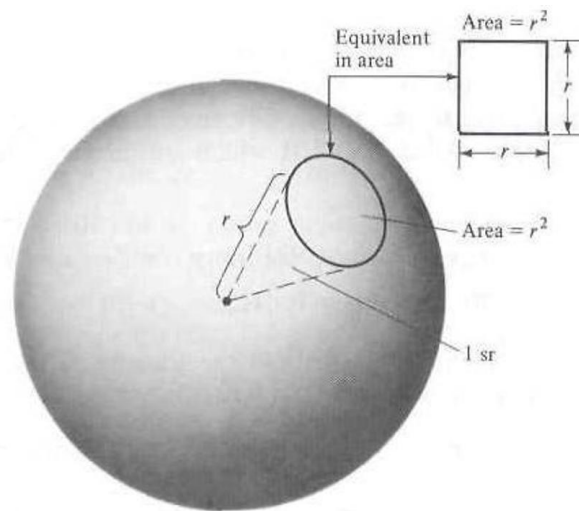
Figure 2.2: Solid Angle[1]

2.4   Directivity

The Directivity is usually defined as being the ratio between the maximum Radiation Intensity and the Radiation Intensity of an isotropic source. This means that this parameter is useful to understand in which direction is the radiated power of an antenna focused on. Mathematically it can be expressed by equation 2.2, in which U is the Radiation Intensity on the direction in which it reaches maximum magnitude.

$$Dmax = \frac{4\pi * U}{Prad} \tag{2.2}$$

2.5   Bandwidth

Bandwidth is an antenna parameter that is related to the frequency range in which the antenna behaves as wanted. For this purpose, the determination of this band, usually takes into account parameters like the Radiation Pattern, Polarization, Radiation Efficiency or Input Impedance. The Bandwidth is usually expressed as a percentage, being that it can be defined by equation 2.3, in which $\triangle f$ is the difference between the limit frequencies of the band and f_0 is the center frequency.

$$BW = \frac{\triangle f}{f_0} * 100 \tag{2.3}$$

2.6   Polarization

Polarization is a property inherent to Electromagnetic Waves that describes the time vari-
ation of the Electric Field Vector (Phase and Magnitude) in the direction of the wave
propagation. As an antenna property, Polarization is determined by the Electromagnetic
Wave associated to its operation when it's radiating/receiving. With this in mind, the Po-
larization of a wave can be described as being: Linear, Circular or Elliptical. One can say
that the Polarization is Linear when the time variation of the Magnitude of the Electric
Field Vector describes a line. On the other hand, if this variation describes a circle, than
the Polarization is said to be Circular. By analysing figure 2.3 one can understand that the
two kinds of Polarization described so far are special cases of Elliptical Polarization. In
fact, it all depends on the ratio between the two Electric Field component vectors aligned
with the axes.
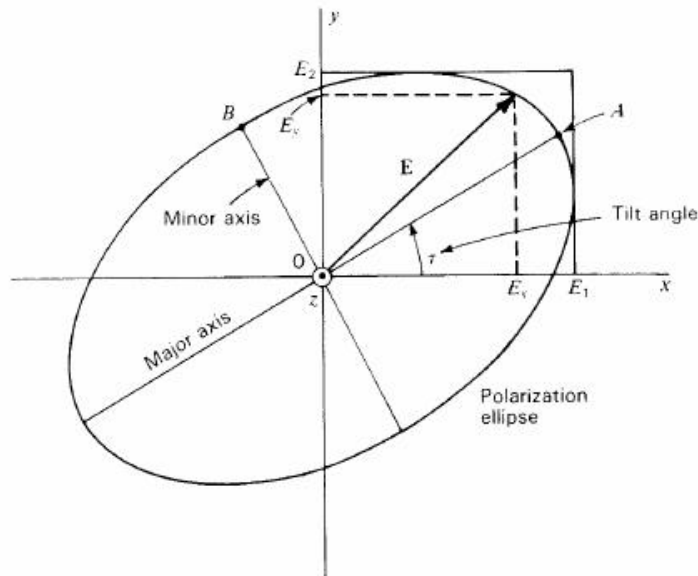
Figure 2.3: Ellipse [2]

As Circular Polarization is particularly interesting for the scope of this thesis, detailed
conditions for it to occur are next presented [1]:

1 The Electric Field must have two orthogonal linear components.

2 The two components must have the same Magnitude and their Phase must differ of
   odd multiples of $\frac{\pi}{2}$.

Another factor that should be taken into account is related to the sense of rotation of
the Electric Field as a consequence of its time variation. By analysing this variation, one
can classify it as being Right Hand or Left Hand. According to the IEEE standard, the

method used to distinguish between these two consists of using the hand that allows, by pointing the thumb finger in the sense of propagation, to rotate the other fingers in the same sense of rotation of the Electric Field Vector. The hand used to do so (Right or Left) determines the sense of the Polarization.

For a better understanding of what was said so far about Polarization, a visual approach is considered in figure 2.4. In this scheme the relation between the orthogonal components of the Electric Field Vector, in terms of Phase and Magnitude, necessary to the existence of the three kinds of Polarization is described.
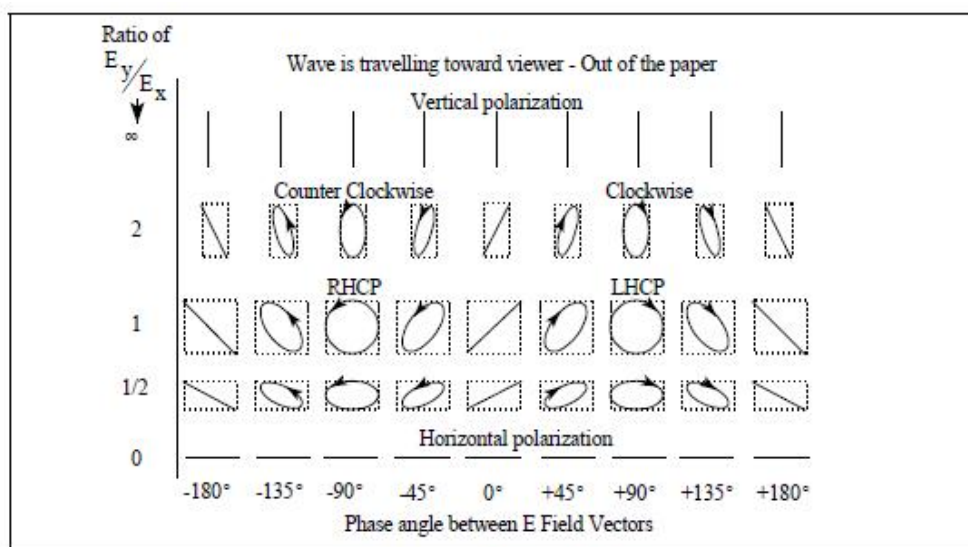
Figure 2.4: The various kinds of Polarization and the relation between the orthogonal components of the Electric Field Vector [3]

There is one final concept related to Polarization that must be introduced here and it's commonly denominated by Polarization Loss Factor. This parameter is a measure of the power loss due to Polarization mismatch (defined in the antenna transmitting mode) between the receiving antenna and the transmitting antenna. Mathematically this loss can be expressed by 2.4. $\widehat{p_w}$ and $\widehat{p_a}$ represent respectively the unit vector of the Electromagnetic Field of the incoming wave and of the receiving antenna. ψ_p is the angle between these two unit vectors. The Polarization Loss Factor is very important and should be taken into consideration specially when doing antenna design. A very important result for this thesis scope, is related to the fact that it can be shown that if both antennas have Circular Polarization with the same sense of rotation, then $PLF = 1$ which means that there are no losses due to Polarization mismatch. The opposite happens if the antennas are Circular Polarized but with different sense of rotation. In such case $PLF = 0$ which means that no power is received.

$$PLF = \left|\widehat{\mathbf{p_w}} \cdot \widehat{\mathbf{p_a}}\right|^2 = \left|cos\psi_p\right|^2 \qquad (2.4)$$

2.7   Input Impedance

Input Impedance is usually associated with the impedance of the antenna's terminals. It's usually composed of a real component and a reactive imaginary component. The resistance, R_a, can be defined as the sum of two components R_r and R_l. R_r is named Radiation Resistance while R_l is the Loss Resistance. A general scheme of the equivalent electric circuit of the antenna in transmitting mode with a generator attached to its terminals is presented in figure 2.5 .
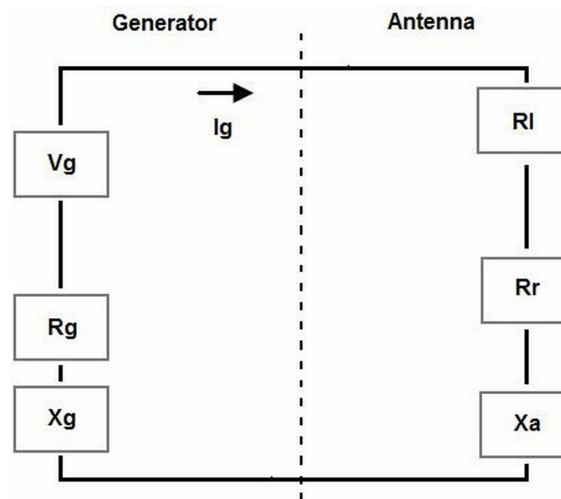
Figure 2.5: Equivalent circuit of the antenna

R_g and X_g are respectively the resistance and the reactance of the generator. X_a represents the antenna reactance and I_g is the electric current that flows in the mesh. It's possible to show that when there is conjugate match of the Input Impedance to the feed line, only 50% of the total power provided by the generator reaches the antenna(the other half are dissipated in the generator resistance). The power dissipated in R_r is the one that will be radiated. It should be pointed out that this electrical scheme is a general one and does not apply to all antennas(e.g. antennas with dielectric losses) but only to very simple ones. It serves however for a general understanding of the antenna functioning.

In this chapter, general antenna concepts with a limited level of detail were presented. It's expected that this way the reader can now understand a bit more about some of the antenna parameters like Polarization, Bandwidth or Radiation Pattern. Although all of these concepts are important for a better understanding of this thesis, particular attention was given to the Radiation Pattern and Polarization. These are in fact particularly important further in this thesis.

Chapter 3

Literature Review

In this chapter several issues related to the development of the subject of this thesis are presented as well as all the theoretical background considered relevant and to them related. The main themes are related to GPS, Small Satellites and their antennas, Microstrip Patch Antennas and Circular Polarized Antenna Arrays.

3.1 Global Positioning System

The GPS is a specific case of a greater group of systems, natives in space, denominated by GNSS. It's their main objective to provide a precise measure of time and positioning. Developed in 1973 by the United States of America Department of Defence, the GPS only became fully operational in 1994. The basis of its functioning involves measuring the time of communication between the satellites (with a very precise internal clock) and the receivers (usually on Earth). By knowing the results of this measurements, as well as the satellite's position, it's then possible to know the distance between this and the receiver. GPS is divided into two main services the Precise Positioning System and the Standard Positioning System. It uses the L band, having by center frequencies $L1 = 1.57542GHz$ and $L2 = 1.2276GHz$. Only the L1 sub-band is used for civil purposes, being that it's used to transmit two main signals named Coarse/Acquisition(C/A) and one other where the Navigation Message is present (see figure 3.1). The first signal mentioned consists "...of a 1023-chip sequence with a period of $1ms$ and a chipping rate of 1.023 MHz" [24], being that in the second one, important technical information for GPS navigation is present.

If it's the case in which the GPS receiver is a LEO satellite, than, considering that it will be freely rotating without any control mechanism, one can expect an Angular Speed in the order of a few rotations per second under no specific axis. If that's so, one can
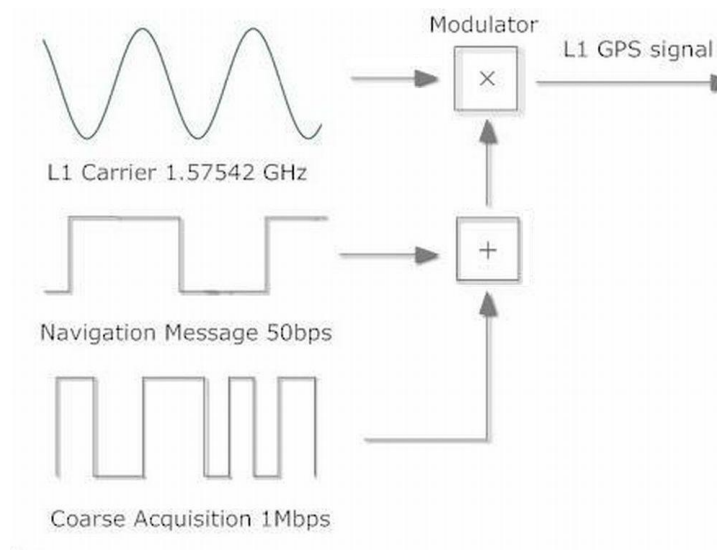
Figure 3.1: Transmitted signals in the L1 sub-band

then assume that situations may happen in which the satellite may lose its GPS signal for periods of time in the order of seconds. As a consequence, there wouldn't be enough measurements to establish a proper GPS communication. With that in mind, the need for a constant and reliable reception is very important for this kind of application. Such reception can only be achieved by the use of an antenna with an adequate Radiation Pattern.

3.2 Small Satellites and Antennas

3.2.1 Introduction

The constant development of new technologies leads to the construction of more and more capable standard satellites, which tend to be more powerful and with higher data rate. At the same time, another kind of satellites, commonly named Modern Small Satellites have been gaining ground. These are much smaller with a mass that is usually a relatively small fraction of that of a standard satellite. In table 3.1 the various sub categories within the small satellite classification are described. These are ordered by mass, cost and the usual time needed to develop the project.

After the finish of what became known as the Cold War, due to economic and political reasons, there was a continuous governmental divestment in space technology in general. This fact along with the advances verified in the Micro-Electronics area as well as in Digital Signal Processing, with the emergence of microprocessors capable of performing complex signal processing operations very quickly, led to the worldwide growing concern for Small Satellite Technology. Although these satellites have been able to perform some complex functions when working together, it should be pointed out that they can't replace

Table 3.1: Satellite Classification [9]

Type	Mass(kg)	Cost (US $)	Time of Development from Proposal to Launch
Conventional large satellite	>1000	0.1-2 B	>5 years
Medium satellite	500-1000	50-100 M	4 years
Mini-satellite	100-500	10-50 M	3 years
Micro-satellite	10-100	2-10 M	1 year
Nano-satellite	0-10	0.2-2 M	1 year
Pico-satellite	<1	20-200 k	<1 year
Femto-satellite	<0.1	0.1-20 k	<1 year

some functions performed by those previously named standard satellites. When high power, high gain antennas or precision pointing are demanded, the latter are required. In [9] some projects using small satellites are described. An example of one of these is The Disaster-Monitoring Constellation. It consists of a six 90 kg micro-satellites constellation, whose purpose is to observe and manage big disasters. It is capable of covering a 600 Km per 600 Km area anywhere on earth and is currently being used by multiple governments such as the UK (country where it was developed), Turkey or China. Another reported example is the Orbiting Pico-Satellite Automated Launcher that was developed at the Stanford University by its students and consists of a 23 Kg Hexagonal Prism. It was fully operational in a LEO for 30 months and it served as a test bed. In this project, a new mission architecture was tested, consisting of a main spacecraft that deployed some smaller spacecrafts in previously determined places in order to perform remote distributed sensing. These are just two successful examples of many that can be found by consulting the appropriated literature. Other examples of applications of these Small Satellites are usually related to:

1. Telecommunications.

2. Space Science.

3. Earth Observation.

4. Military or educational applications.

3.2.2 The Vorsat Project

The Vorsat Project consists on the design and implementation of a CubeSat to be deployed in a LEO, whose main goal is to test and study the atmospheric re-entry, as well as, the ability to recover a capsule. The CubeSat is a specific kind of pico-satellite whose volume is $10 * 10 * 10\ cm^3$ and whose mass is inferior to 1 Kg. This kind of satellite has been

receiving much attention all over the world. Due to its reduced conception time and cost, it presents itself as a cost-effective solution for universities and countries with no financial capability to develop a standard space program, as it allows amongst other things, all kind of scientific experiments. The general abilities/systems of CubeSats when compared to standard satellites are as follows [4]:

1 Power System usually based on solar panels and batteries.

2 Data Processing and Storage Unit.

3 Uplink/Downlink Communications.

4 Attitude Determination and Control.
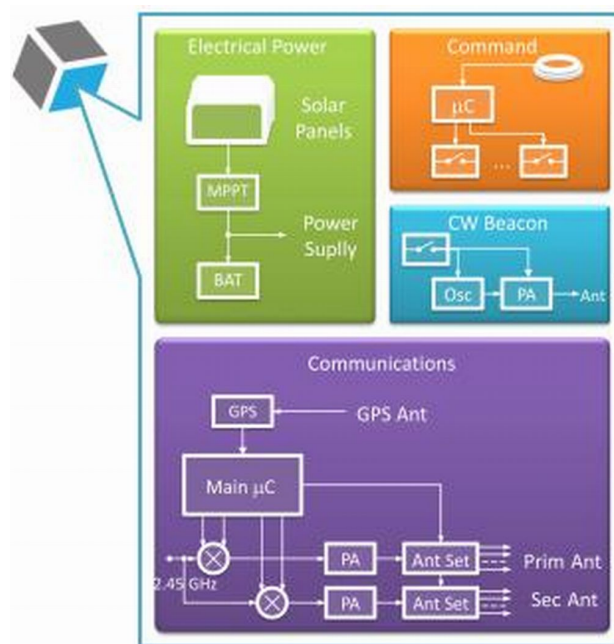
Figure 3.2: Draft of the Vorsat structure [4]

The great majority of the space missions involving CubeSats use, as a mean for launch and deployment, the Poly-PicoSatellite Orbital Deployer. This consists briefly in a rocket on which the CubeSats are attached to, being that it deploys them into orbit once it receives a proper signal indicating that it has reached a pre-determined altitude. In the Vorsat case, the idea is for it to be launched as a part of a bigger project named QB-50. This project involves the ESA and NASA, as well as the Von Karman Institute. The objective is to launch 50 CubeSats into a LEO, in order to study "in situ the temporal and spatial variations of a number of key constituents and parameters in the lower thermosphere (90-320 km) with a network of 50 double CubeSats, separated by a few hundred kilometres and
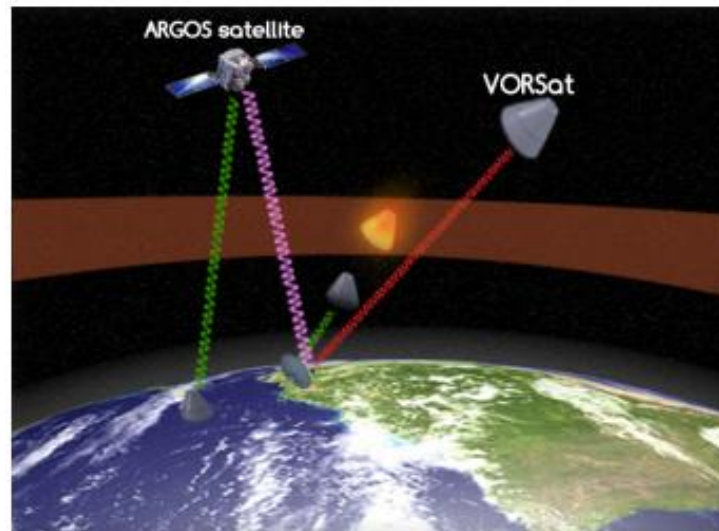
Figure 3.3: Vorsat's re-entry scheme [5]

carrying identical sensors." [25]. The general structure of the initial Vorsat project can be seen in figure 3.2. From this figure, it's possible to observe that the CubeSat is divided into four main sub-systems, all related to what have been already described to be some of the general abilities/systems expected for this kind of satellite. Further description of the functioning of this satellite won't be performed as it's considered not to be so relevant for the purposes of this thesis. However, one of the subsystems previously showed, has a direct interest to the scope of this thesis, being that the Communications one. In fact, as can be seen, an integral part of this system is the GPS receiving antenna, developed as an end product of this thesis. Now that a bigger insight about this project was given, it's possible for the reader to understand the importance of this component for the success of this project mission. In fact, this antenna's purpose is to provide the Vorsat a GPS signal from time to time, and so supplying it with accurate time, position and velocity measurements, in order for the satellite to be able to locate itself precisely, when in orbit. The constraint of periodic GPS measures is related to power save measures, and as a consequence, during the time between measures, the satellite will be performing an estimation of its orbit position. Moreover, the atmospheric re-entry trajectory control system, will also find the GPS measures useful, as it will rely on them until the antenna burns out. A draft of this re-entry can be seen in figure 3.3. The ARGOS system will be used to locate the capsule once it lands.

3.2.3 Small Satellite GPS Antennas

In the last couple of years, small GPS antennas have been receiving a lot of attention. A few different designs have been applied to this purpose. In this case, these antennas

have to be able to comply not only with the GPS standard but also with the conditions inherent to this kind of application. In [9], a number of characteristics/items to be taken into consideration due to the conditions in which Small Satellites antennas operate are described:

1 High reliability, since there are no maintenance opportunities.

2 Small dimensions, low mass and high efficiency with a low production cost for a small satellite and a low budget.

3 Mechanical robustness in order to survive the launch.

4 Assurance of good operation on a big range of temperatures that can go from -150ºC to 150ºC.

5 The harsh radiation environment, the effect of atomic oxygen (only for LEO deployment missions) and micro-gravity and vacuum effects on the constituent materials of the antenna must be taken into account.

6 Another important effect that must be considered is the interaction amongst the antennas and between these and the satellite structure. In fact, the latter can cause electromagnetic scattering, resulting in the degradation of the Radiation Pattern. This effect is particularly harmful since the existence of nulls in the pattern can cause important data to be lost. To try to study and minimize this effect, it's common nowadays to use EM software simulators and/or to perform practical measurements.

Also the GPS standard imposes some restrictions to the antenna performance. In fact, this antenna must operate in the GPS frequency band ($L1 = 1.575GHz$ and $L2 = 1.227GHz$), have low backward radiation and it must have Right-Hand Circular Polarization. Moreover, Good Cross Polarization Rejection and a Sharp Pattern Slope for Low Elevation Angles are desirable in order to avoid Multipath Errors. These consist on the arrival of a signal over more than one direction and are due to reflections. These errors tend to be the most relevant ones since they usually give origin to signals that cannot be filtered using signal processing methods in the receiver. The most problematic of these are due to reflections that happen in the surfaces near the antenna, resulting in signals whose path exceed the direct one by less than 10 meters [10]. An illustration of this phenomenon is presented in figure 3.4. Taking these needs into consideration, a couple of antennas appear as suitable solutions.

3.2.3.1 Examples of Small Satellite GPS Antennas

The use of GNSS for small satellites began at the University of Surrey (UK). This university's early research regarding Small Satellites led to the creation of a spin-off company named Surrey Satellite Technology Ltd, which later became an established leader
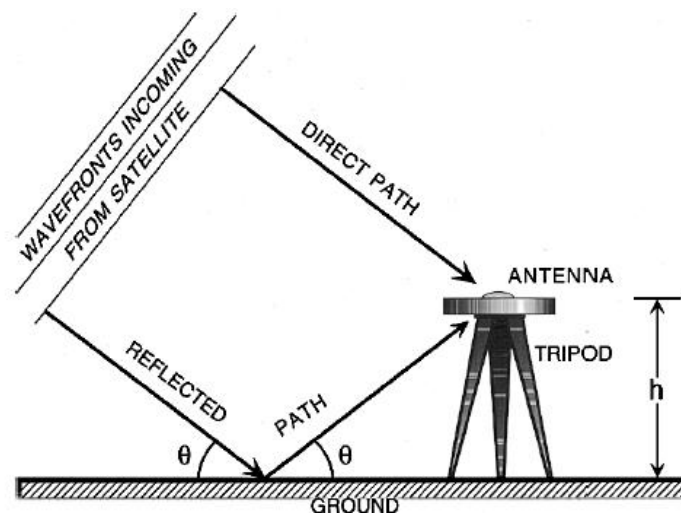
Figure 3.4: Scheme of the Reflections that lead to Multipath Errors [6]

in its area of expertise. They offer several GPS integrated solutions (GPS Receiver plus Antenna(s) plus add-ons) for various applications related to small satellites localization, with a price range that goes from 15000 to 252000 dollars [7]. In general, all of these solutions use Active Patch Antennas with exception of the cheapest one that offers as an alternative the Active Quadrifilar Helix Antenna. Examples of both of these can be seen in figure 3.5.

Figure 3.5: Example of a Patch Antenna on the left and of a Quadrifilar Helix Antenna on the right [7]

Quadrifilar Helix Antennas and now also Printed Quadrifilar Helical Antenna have become one of the main solutions when it comes to small satellite GPS Receivers. This antenna distinguish itself by "...its cardioid pattern, circular polarization and logical size compared to other antennas. In particular, the cardioid pattern is the favourite pattern for LEO satellite antennas" [8]. The main difficulty when using this kind of antenna for this purpose, is to implement the dual-frequency resonant behaviour. There are some

options when it comes to create this kind of behaviour, all of them with some advantages and disadvantages. In the Quadrifilar Helix Antennas case, the dual-frequency operation involves the use of two different concentric antennas [26]. The Printed Quadrifilar Helical Antenna achieves multiple-frequency operation through the variation of the number and length of the thin arms as well as the coupling between them. In figure 3.6, illustrative schemes of these printed antennas can be seen. This kind of cylindrical shaped antenna consists generally in a thin dielectric with four printed helix-shaped radiating elements.

Figure 3.6: From the left to the right a scheme of a single, double and triple frequency band Printed Quadrifilar Helical Antenna [8]

Another already referred class of antennas, which is nowadays one of the most popular and well documented ones, is the Microstrip Patch Antenna. It consists generally in a radiating element, printed on a thin substrate that separates it from a ground plane. This kind of antenna is usually preferred for its low profile, easy fabrication and hemispherical radiation pattern. Circular Polarization is usually implemented by properly selecting the feed point or the antenna's radiating element shape. The dual-frequency behaviour is usually achieved using stacked-patches. An example of one of these antennas is the one built by RUAG Aerospace Sweden. This antenna consists in a Patch Excited Cup, as can be seen in figure 3.7. This is made up by two Circular Patches in a circular cup with a 16 cm diameter. It radiates within $+/-80^{\circ}$ in the zenith direction and has low backward radiation. The bottom patch is capacitively fed by four probes, in order to achieve resonance in both $L1$ and $L2$ sub bands.

An alternative to the previously presented design is the special configuration consisting on a Shorted Annular Patch Antenna (see figure 3.8). It has been reported in [10], [27]. According to the authors, this antenna appears as a good solution when compared to other high performance commercial GPS antennas because it's thought to diminish multipath errors as much as possible, making it attractive for space applications.

Due to its circular polarization response, another sort of antenna is proposed in [12]. It's called Conical Spiral Antenna and an example of one of these can be seen in 3.9. The
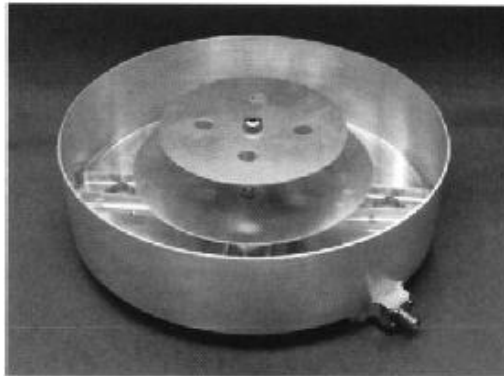
Figure 3.7: RUAG Aerospace Sweden GPS Stacked-Patch Antenna [9]
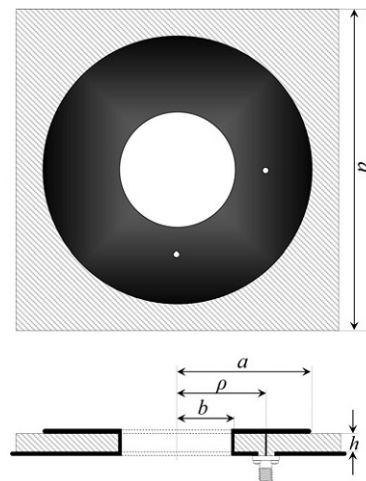
Figure 3.8: Shorted Annular Patch Antenna General Scheme [10]

size of both the diameter of the base and the vertex of the cone determine the Bandwidth.

To sum up, in [12] a comparison is made between the antennas here presented, in order to figure out which one would be the most appropriate for GPS applications. The first antenna to be analysed was a Microstrip Patch Antenna. Good results were obtained when using single frequency, with a Cross Polarization Rejection Ratio of -17 dB. However, when using a Stacked Patch Antenna, composed of two patch antennas for dual frequency operation, this parameter drops drastically to less than -5 dB in both $L1$ and $L2$. With this in mind we can conclude that this kind of antenna has a very good behaviour in single frequency operation, being however that the same does not happen when it comes to dual frequency operation. The next analysed antenna was the Quadrifilar Helical Antenna, which proved to have a good behaviour when it comes to multipath errors rejection. The main problem of this configuration is related to the Radiation Patterns (L1 and L2) of the dual frequency operation as they have some compromising differences. Finally, the antenna with the best overall results was the Conical Spiral Antenna, as it fulfilled all the
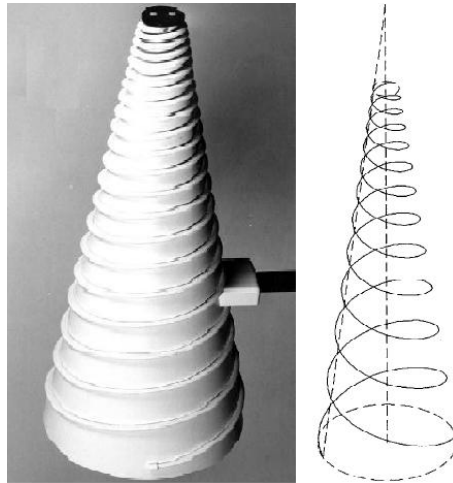
Figure 3.9: Conical Spiral Antenna Example [11],[12]

needs in all the parameters relevant for GPS operation. Moreover, the authors used a lossy absorbing material which resulted in a huge reduction of the front-to-back radiation ratio to less than -15 dB.

3.2.3.2   Examples of General Purpose Low Cost Substrate GPS Patch Antennas

Due to the easiness of Microstrip Patch Antennas fabrication, and their good GPS single frequency behaviour, they will be the subject of further investigation here. In particular, and due to the academic nature of this project and thesis, Low Cost Substrate GPS Patch Antennas are particularly interesting, since one of the main low cost substrates investigated in literature is FR-4. This material, commonly used for PCB fabrication appears as a good solution for prototyping and is normally abundant in the faculty workshops. Some research has been done in the subject here in discussion, [13], [14]. According to the authors, the use of low cost substrates, particularly FR-4, brings some more complexity to the antenna design. This is mainly due to:

1 The inhomogeneity and inaccuracy of the FR-4 relative permittivity (around 4.4 at $L1$ frequency).

2 The substrate high loss tangent (around 0.02).

The first mentioned problem is particularly harmful since it will result in a resonant frequency shift. In order to compensate this, the authors suggest the introduction of four stubs in the corners of the Circularly Polarized Square Truncated Corner Microstrip Antenna, as shown in figure 3.10. The design of these stubs is done using HFSS (Full-Wave electromagnetic field software), being the objective the optimization of the Axial Ratio.
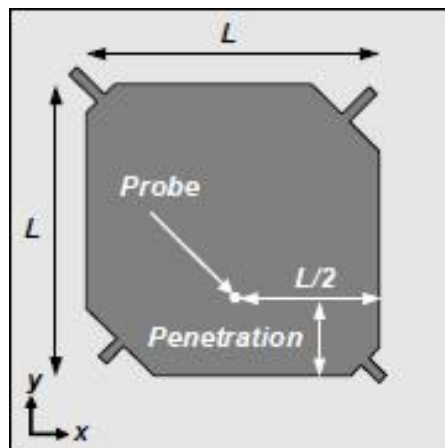
Figure 3.10: General Scheme of a Low Cost Circularly Polarized Square Truncated Corner Microstrip Antenna with four stubs as proposed by [13]

The first prototype built in [13] was with a 1.524 mm thickness substrate. Good results were achieved in all parameters (Input Impedance, Axial Ratio Magnitude and Bandwidth) except for the Radiation Efficiency which proved to be extremely low (34%). With that in mind, the substrate thickness was augmented to 6.2 mm, which raised the Radiation Efficiency to 74% at the expense of an unacceptable inductive level of impedance. This was solved efficiently by opening a Fractal Gap, as shown in figure around the feed 3.11.
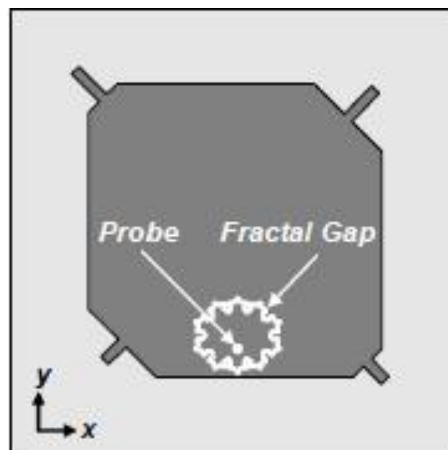
Figure 3.11: Truncated Corner Microstrip Antenna with a Fractal Gap to compensate the inductive level of the impedance as proposed by [13]

An alternative simpler solution to this problem is proposed in [14], where a rectangular topology is used instead of the square one. This way, a very good antenna was obtained with an acceptable Radiation Efficiency of 67%. A scheme of this antenna is presented in figure 3.12.
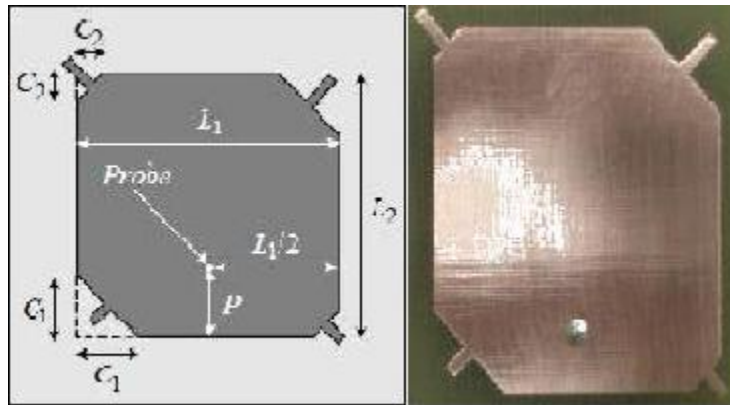
Figure 3.12: On the left a scheme of the antenna proposed by [14] with the following measures L1=41 mm,L2=43.35 mm,C1=10 mm,C2=4 mm,P= 7,675 mm, length of major stub= 5.5 mm, length of minor stube=3.5 mm. On the right an example of one of this antennas applied to the GLONASS system [15]

3.3 Microstrip Patch Antennas

3.3.1 Introduction

The first theoretical developments in the history of Microstrip antennas were made during the fifties. However twenty years passed before theory was put into practice with the development of the first antennas of this kind. This delay was due to the lack of some technological and theoretical resources, e.g. low loss substrates or accurate theoretical models.

In figure 3.13 one can see the general scheme of a Microstrip Patch Antenna. It's generally composed by a thin metal layer (the thickness is very small when compared to the vacuum wavelength λ_0) usually referred to as Patch, which is usually located between 0.3% to 5% of the vacuum wavelength above the ground plane. Between these two planes there is a dielectric with a typical Relative Permittivity between 2.2 and 12. Both the dielectric thickness h and its Relative Electric Permittivity ε_r have a major influence in some of the characteristics of the Microstrip Antenna. In specific, thicker substrates with low ε_r lead for example to a better Radiation Efficiency, bigger Bandwidth and to a larger Patch. The opposite happens when one uses thinner substrates with low Relative Permittivity, being that this fact is usually used to lower the antenna's size.

The radiating element (Patch), can assume many geometric forms. The most common are square, rectangular, circular or elliptical, triangular-shaped or toroidal. These forms are preferred mainly because they are simpler to analyse and to build. Next, some general characteristics of this kind of antenna are presented [16].

1   Can be used in frequencies ranging from 100 MHz to 50 GHz.
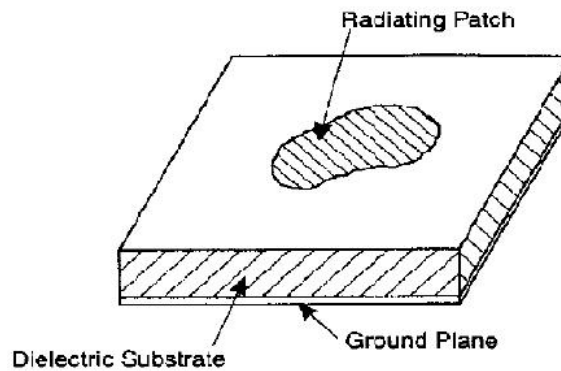
Figure 3.13: General Structure of a Microstrip Patch Antenna [16]

2 Low weight and volume. Mechanical robustness if mounted on hard surfaces.

3 Low manufacturing cost.

4 Possibility of implementing various types of Polarization using simple feeding schemes.

5 Easy integration with microwave circuits.

Some of the negative characteristics of this kind of antenna are: Low Gain($-6dB$), narrow Bandwidth, low Polarization purity and Surface Wave creation. There are however many ways to mitigate some of these problems. However that is usually only possible at the expense of others. It's up to the designer to understand which are the most important antenna parameters to that particular application.

3.3.2 Feeding Methods

There are several supply schemes for Microstrip Patch Antennas. These are usually divided into Contact methods or Non Contact methods. For the first case, there is a feeding structure that connects directly to the Patch. In the second case, the feed occurs through Electromagnetic Coupling, i.e. without any physical contact with the Patch. There are four main methods commonly reported in literature. Advantages and disadvantages of these are presented in table 3.2.

From the four feeding methods presented, the first two belong to the first previously mentioned group, while the others are Non-Contact schemes. In figure 3.14 the four mentioned methods are shown. On the top left corner there is an example of Microstrip Line feeding. It's noticeable that the width of the conductor is much smaller when compared to the Patch dimensions. At its side a Coaxial Feed Line is illustrated where the side view shows how this works. The inner conductor connects directly to the Patch while the external one is connected to the ground plane. Immediately below the Aperture Coupling

Table 3.2: Feeding Methods

Feeding Method	Advantages	Disadvantages
Microstrip Line	Easy manufacturing and modelling. Easy matching of Input Impedance.	Thick substrates lead to a Surface Waves raise, limiting the Bandwidth. Increased Cross Polarization.
Coaxial Line	Easy manufacturing. Easy matching of Input Impedance.	Limited Bandwidth and difficult modelling, particularly for thick substrates. Increased Cross Polarization.
Aperture Coupling	Easy modelling. Good Polarization purity.	Limited Bandwidth and difficult implementation. Lower Cross Polarization.
Proximity Coupling	Increased Bandwidth and easy modelling. Easy matching of Input Impedance.	Hard to manufacture.

is illustrated. It consists of two substrates separated by the ground plane. In addition there is a Microstrip Line in the bottom side of the bottom substrate which passes its energy to the Patch by Electromagnetic Coupling through a hole in the ground plane. Finally, in the Proximity Coupling scheme the Microstrip Line feed is located between the two substrates.

Along with the advantages and disadvantages of each of the Feeding Methods previously presented, there's also another very important constraint that should be taken into consideration that is related to the feasibility of the scheme in physical terms, when inserted into the bigger system which the antenna is part of.

3.3.3   Analysis of a Rectangular Microstrip Patch Antenna

3.3.3.1   Introduction

Throughout the years many analysis methods for Microstrip antennas were developed. All of these have the common objective of predicting several parameters related to this kind of antenna such as Radiation Pattern, Gain, Polarization, etc. The difficult analysis of this kind of antenna is due not only to the fact that there is no homogeneity in the boundary conditions, but also due to the variety of feeding methods and of Patch shapes. The analysis methods can be divided into two groups: The Analytical Methods and the Full-Wave Methods. The most commonly used methods from the first group are the Transmission Line Model and the Cavity Model. The other group is based on the solution of "Maxwell's Equations", using numerical methods such as Finite Difference Method, the Finite Element Method or the Method of Moments. The big difference between these two groups is that the methods of the former are simpler and less accurate compared to
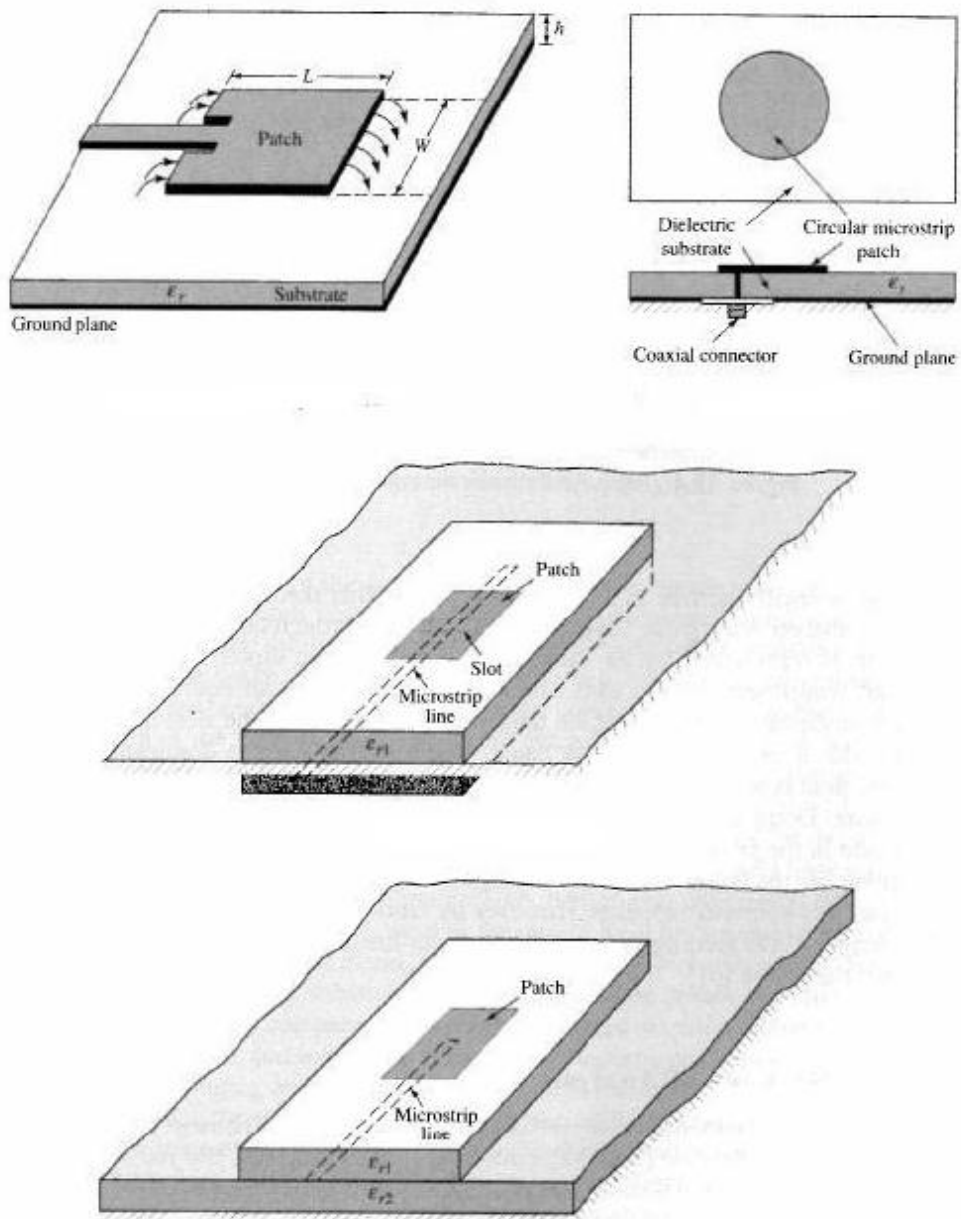
Figure 3.14: The four most common Feeding Methods [1]

those of the second. The Analytical Methods are generally used to obtain CAD formulas, in order to have an initial idea of some of the antenna parameters. After that, the analysis typically relies on simulation software based on a Full-Wave analysis.

In general terms, the Model of Transmission Line is the simplest to interpret, giving enough information about the physical parameters of the antenna. However this model has some limitations. In fact, not only it isn't a very precise method, but also it's only applicable to the Rectangular Patch. Within the so-called analytical models, there is also
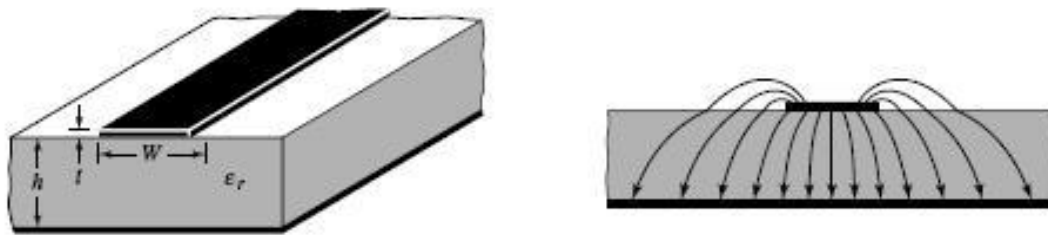
Figure 3.15: A Microstrip Line is shown on the left while on the right Electric Field Lines are presented [1]

the Cavity Model, which exchanges some complexity for greater accuracy. This model can be used for the analysis of regular geometric forms of the Patch, and for the analysis of circular polarization. In a brief note, it's also important to highlight some commercial programs that perform a Full-Wave analysis, such as HFSS or CST Microwave Studio. These differ among other things in the method used, for example the HFSS is based on the Finite Element Method. That said, a better description of the two Analytical Methods is presented. Due to reasons related to the scope of this thesis, this analysis is focused in a Rectangular Microstrip Patch Antenna. Also most of the literature researched did this specific analysis. The one here presented is based on the one from [1] since this analysis presented itself as brief, and more design oriented.

3.3.3.2 Transmission Line Model

The use of a Transmission Line Model for this type of antenna seems an obvious choice, and so it serves as a first approach. It models the antenna as consisting of two slots separated by a transmission line of length L and impedance Z_c. In figure 3.15, one can perceive a Microstrip Line, as it was previously described. In the diagram on the left a general scheme represents the Radiated Electric Field Lines. As it's represented, the fact that the Patch has limited physical dimensions has consequences in the radiated fields. In fact, these fields undergo Fringing, i.e. the fields propagate outside the dielectric. It's known that the Fringing Effect is function of the Patch dimensions, substrate thickness, Relative Permittivity of the substrate and frequency. This effect will result in the existence of two dielectrics, i.e. the air and the substrate. Taking into account that the Relative Electric Permittivity of the air is nearly one, and so usually less than that of the substrate, the Effective Relative Electric Permittivity(ε_{reff}) is comprised between 1 and the Relative Electrical Permittivity of the Substrate. The larger the ε_r and the Patch dimensions when compared to the substrate thickness h, the closer ε_{reff} gets to ε_r. The same happens when frequency is increased.

A formula to calculate ε_{reff}, accurate for low frequencies is given by 3.1.
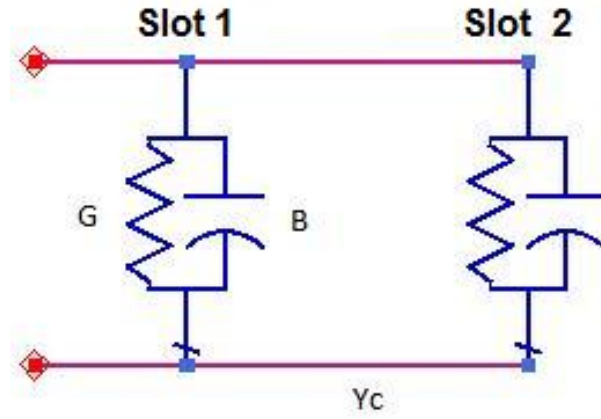
Figure 3.16: Rectangular Microstrip Patch Antenna Transmission Line Model

$$\varepsilon_{reff} = \frac{\varepsilon_r + 1}{2} + \frac{\varepsilon_r - 1}{2}\left(1 + 12\frac{h}{W}\right)^{-\frac{1}{2}} \qquad (3.1)$$

The Fringing Effect, makes the antenna electrically bigger than what was supposed to be by taking into account only its physical dimensions. To make this taken into consideration, an empirical formula was created 3.2, [28]. In this equation, $\triangle l$ is the length extension to be considered for each extremity of the Patch.

$$\triangle l = 0.412h\frac{(\varepsilon_{reff} + 0.3)(\frac{W}{h} + 0.264)}{(\varepsilon_{reff} - 0.258)(\frac{W}{h} + 0.813)} \qquad (3.2)$$

With this in mind, a new parameter called Effective Length is considered $L_{eff} = L + 2\triangle l$. From the Cavity Model, and assuming X as being the dimension normal to the Patch, the frequency of resonance for the TM_{10} mode can be defined by equation 3.3, in which v_0 is the vacuum light speed.

$$fr_{10} = \frac{v_0}{2L\sqrt{\varepsilon_r}} \qquad (3.3)$$

It's now possible to enter Fringing effect in the resonant frequency calculus through equation 3.4.

$$frc_{10} = \frac{v0}{2(L + 2\triangle l)\sqrt{\varepsilon_{reff}}} \qquad (3.4)$$

According to the Transmission Line Model, the Rectangular Microstrip Patch antenna can be represented by 3.16. In this figure, each one the two slots is modelled by an admittance Y.

That said, if Y_1 and Y_2 are respectively the admittances corresponding to two slots, and assuming that these are equal, then it follows that $Y_1 = Y_2 = G + jB$. Modelling each slot

as being uniform and infinite in a perfect plane conductor (see figure 3.17), then come
the equations 3.5 and 3.6, both of them derived in the book already referred as being the
basis of this sub chapter.
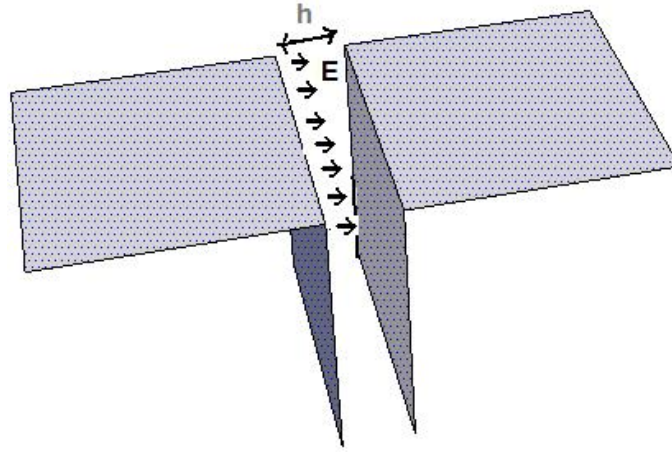
Figure 3.17: Slot Model in a perfect plane conductor

$$G = \frac{W}{120\lambda_0}\left(1 - \frac{1}{24}(k_0 h)^2\right) \qquad \frac{h}{\lambda_0} < \frac{1}{10} \qquad (3.5)$$

$$B = \frac{W}{120}\left(1 - 0.636 ln(k_0 h)\right) \qquad \frac{h}{\lambda_0} < \frac{1}{10} \qquad (3.6)$$

From the Transmission Line Model, one can obtain an approximate value of the Input
Impedance of a Rectangular Microstrip Patch Antenna. To this end, it's necessary to move
the admittance of the second slot to the output terminals, doing so by using the Equations
for Admittance Transformation for Transmission Lines. If this is done, it is concluded
that at the resonant frequency $Y_2 = G - jB$, resulting in a purely real Input Impedance
given by 3.7. Despite the fact that the mentioned equation does not take into account the
mutual effects between the two slots, it gives a reasonable approximation in exchange for
low mathematical complexity. From this equation one can conclude that in a Rectangular
Patch, the magnitude of the Input Impedance is inversely proportional to the Width of the
Patch.

$$R_{in} = (2G)^{-1} \qquad (3.7)$$

Finally it's also important to understand how does the Input Impedance varies with the
feed position. To do so,[1] derives equation 3.8 which was thought for the case in which
the feed is done by a Microstrip Line. y_0 is the distance along the length of one end of the
"Patch" towards the opposite end. In figure 3.18, it's possible to understand that the Input

Impedance is maximum at the extreme points along the length of the Patch, reaching a minimum in the middle.

$$R_{in}(y_0) = cos^2(\frac{\pi}{L}y_0)(2G)^{-1} \tag{3.8}$$
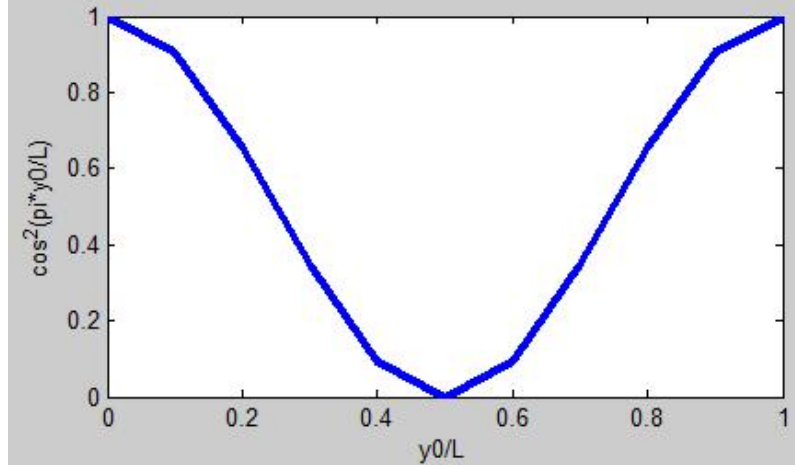
Figure 3.18: Input Impedance vs Feed Position.

3.3.3.3 Cavity Model

This model analyses the antenna as being a resonant cavity (see figure 3.19). This cavity is filled by the dielectric, bounded by perfect electric conductors at the top and bottom, and in the periphery along the perimeter perfect magnetic conductor walls are assumed. This last assumption is the more valid the smaller the ratio of substrate thickness and width of the Patch. Moreover, a thin substrate, approaches the Patch and the ground plane, diminishing the Fringing effect, resulting in a Electric Field normal to the radiator. This way, only TM^x modes are considered. It should also be pointed out that in order to model the irradiation in the Cavity Model, it's necessary to create a loss mechanism. To this end, a parameter named Effective Tangent Loss δ_{eff} is created.

Using the Vector Potential method, one can reach the following equations 3.9.

$$
\begin{aligned}
\mathbf{E_x} &= -j(\omega\mu\varepsilon)^{-1}\left(\frac{\partial^2}{\partial x^2}+k^2\right)\mathbf{A_x} \\
\mathbf{H_x} &= 0 \\
\mathbf{E_y} &= -j(\omega\mu\varepsilon)^{-1}\left(\frac{\partial^2\mathbf{A_x}}{\partial x\partial y}\right) \\
\mathbf{H_y} &= \frac{1}{\mu}\frac{\partial\mathbf{A_x}}{\partial z}
\end{aligned}
$$
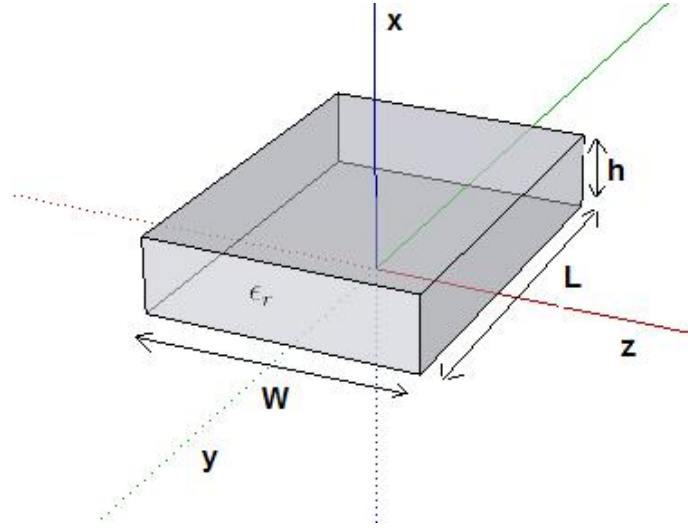
Figure 3.19: Cavity Model Scheme

$$
\begin{aligned}
\mathbf{E_z} &= -j(\omega\mu\varepsilon)^{-1}\frac{\partial^2 \mathbf{A_x}}{\partial x \partial z} \\
\mathbf{H_z} &= -\frac{1}{\mu}\frac{\partial \mathbf{A_x}}{\partial y}
\end{aligned}
\tag{3.9}
$$

In these equations, the vector potential $\mathbf{A_x}$ is the solution of the wave equation $\bigtriangledown^2\mathbf{A_x} + k^2\mathbf{A_x} = 0$ in which k is the wavenumber. If the boundary conditions are taken into account, one can reach equation 3.10. x', y' and z' are the spatial coordinates of reference point, A_{mnp} represents the amplitude of each mode, $k_x = m\frac{\pi}{h}$, $k_y = n\frac{\pi}{L}$ and $k_z = p\frac{\pi}{W}$.

$$
A_x = A_{mnp}cos(k_x x')cos(k_y y')cos(k_z z')
\tag{3.10}
$$

Substituting 3.10 in 3.9, equations 3.11 are obtained for the multiple components of the Electric and Magnetic Fields in the cavity.

$$
\begin{aligned}
\mathbf{E_x} &= -j\frac{(k^2 - k_x^2)}{\omega\mu\varepsilon}A_{mnp}cos(k_x x')cos(k_y y')cos(k_z z') \\
\mathbf{H_x} &= 0 \\
\mathbf{E_y} &= -j\frac{k_x k_y}{\omega\mu\varepsilon}A_{mnp}sin(kx'_x)sin(k_y y')cos(k_z z') \\
\mathbf{H_y} &= -\frac{k_z}{\mu}A_{mnp}cos(k_x x')cos(k_y y')sin(k_z z') \\
\mathbf{E_z} &= -j\frac{k_x k_z}{\omega\mu\varepsilon}A_{mnp}sin(k_x x')cos(k_y y')sin(k_z z') \\
\mathbf{H_z} &= \frac{k_y}{\mu}A_{mnp}cos(k_x x')sin(k_y y')cos(k_z z')
\end{aligned}
\tag{3.11}
$$

Another important equation that allows the calculation of the resonant frequency for each mode is given by 3.12.

$$f_{rmnp} = (2\pi\sqrt{\mu\varepsilon})^{-1}\sqrt{(\frac{m\pi}{h})^2 + (\frac{n\pi}{L})^2 + (\frac{p\pi}{W})^2} \qquad (3.12)$$

From 3.12, it's possible to calculate the resonant frequency of the dominant mode (lowest frequency mode). Taking into account that the substrate thickness is always lower than the length and width of the Patch, than the dominant mode is TM_{010}^x and its resonant frequency is $f_{r010} = \frac{v0}{2L\sqrt{\varepsilon_r}}$. It's important to notice that in the case of a square Patch, both the modes TM_{010}^x and TM_{001}^x would have the same resonant frequency. This fact is the theoretical base to the majority of the researched methods to create Circular Polarization.

From equations 3.11 and $k_r^2 = w_r^2\mu\varepsilon$, one can conclude that for the TM_{010}^x mode, the Electric and Magnetic Field is mathematically described by 3.13 being that $\mathbf{E_0} = -jwA_{010}$.

$$\mathbf{E_x} = \mathbf{E_0}cos(\frac{\pi}{L}y')$$
$$\mathbf{H_z} = \mathbf{H_0}sin(\frac{\pi}{L}y')$$
$$\mathbf{E_y} = \mathbf{E_z} = \mathbf{H_x} = \mathbf{H_y} = 0 \qquad (3.13)$$

Graphically, these can be seen in figure 3.20, as both principal planes are represented(E plane(on the left) and H(on the right)).
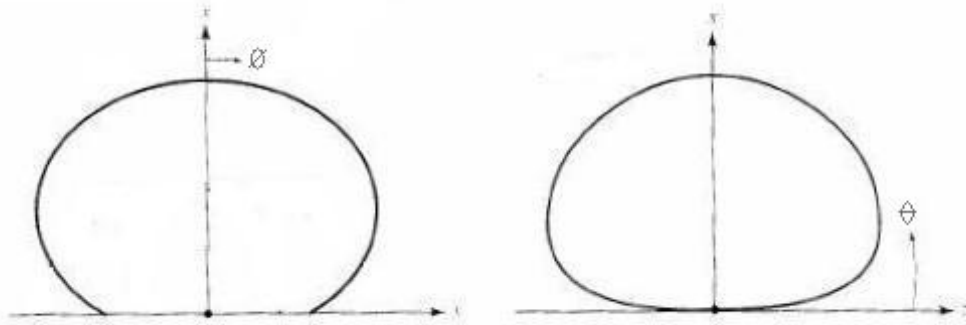
Figure 3.20: Typical Radiation Pattern for both principal planes: E and H [1]

In order to determine the Electromagnetic fields in the Far-Field region, it's deduced in [1] an Equivalent Density Current Model, as can be seen in 3.21. The electric current density $\mathbf{J_t}$ which is intended to include the presence of the Patch in this model is negligible due to the low thickness of the substrate. The electric current density $\mathbf{J_s}$ can also be assumed as zero, as the magnetic fields along the perimeter of the cavity are approximately
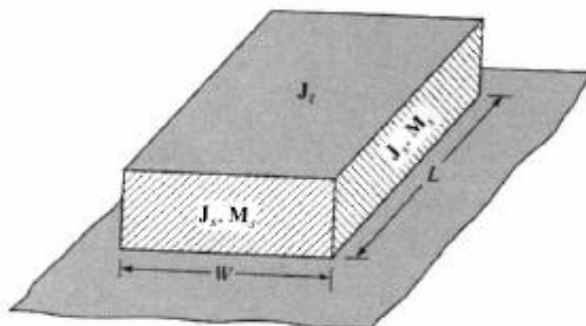
Figure 3.21: Current Density Model [1]

zero. Finally, only the magnetic current density is left $\mathbf{M_s}$. Taking into account the ground plan and by using the Method of Images, equation $\mathbf{M_s} = -2\hat{n} \times \mathbf{E_a}$ is established, being that $\mathbf{E_a}$ is the Electric Field of the four boundaries of the cavity. These four are modelled as being perfect magnetic conductors and are here assumed as radiating slots. One can also conclude that for the case here in analysis (Rectangular Patch), the two boundaries along the length radiate, while the radiation of the two other along the width is negligible. These two groups are distinguished in literature as radiating and non radiating slots.

Finally the equations regarding the Electric Field of the radiating slots in the Far-Field region are presented in 3.14. In these equations $V_0 = E_0 h$ and r is the distance to the reference point.

$$\mathbf{E_r} \simeq \mathbf{E_\theta} \simeq 0$$

$$\mathbf{E_\phi} = \frac{jk_0 V_0 W e^{-jk_0 r}}{\pi r} (sin(\theta) \frac{sin(X)}{X} \frac{sin(Z)}{Z})(cos(\frac{k_0 L_e}{2} sin(\theta) sin(\phi)))$$

$$X = \frac{k_0 h}{2} sin(\theta) cos(\phi)$$

$$Z = \frac{k_0 W}{2} cos(\theta) \tag{3.14}$$

3.3.4 Methods to Create Circular Polarization

Circular Polarization can be created in many ways in different kinds of Microstrip Patch Antennas. In the context of this dissertation, only Rectangular/Square Patch antennas will be studied. This is due to the fact that these are the most common, well documented and simple kind of antennas when it comes to Circular Polarization creation. If no change is applied to this kind of antenna it radiates essentially Linearly Polarized waves. It's known that Circular Polarization is characterized by an Electric Field with two linear orthogonal components, with the same magnitude and a phase shift of 90º. In general, this can

be obtained by changing the physical structure of the Patch or its feed position or both. Specifically, there are two kinds of common methods to create this kind of Polarization: single-feed or multi-feed. In both cases, the general idea is to excite the TM_{10} and TM_{01} modes (Z dimension was assumed as being in the normal direction to the Patch).

Thus, possibly the most obvious method consists in feeding a square Patch in two different points in adjacent sides of the Patch(see figure 3.22). In this case, it's necessary to use some technological means to create the necessary 90º phase shift. To do so, Power Dividers or 90º Hybrids are usually utilized.
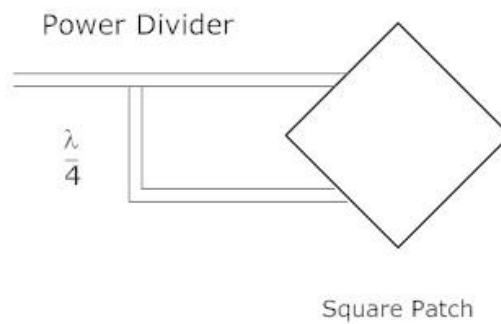
Figure 3.22: Double-feed scheme

The previously mentioned double-feed method has a big disadvantage of needing auxiliary equipment to perform the phase shift. Alternatively, single-feed methods seem to overcome this issue. In fact, according to [1], the general concept of this kind of method is to excite two orthogonal degenerate modes of equal amplitude by placing the feed in a proper place. This degeneracy is solved by introducing perturbations in the cavity, e.g. using an almost square Patch(one side is slightly bigger than the other), cutting small sections of the Patch, etc.

One first method uses an almost square Patch being that the feed position is along one of the Patch's diagonals as can be seen in figure 3.23. The diagonal chosen determines if the Polarization is Right-Hand or Left-Hand. In the figure, the scheme on the left corresponds to Left-Hand Polarization while the one on the right corresponds to Right-Hand Polarization.

Assuming X as being the direction normal to the antenna, as it happens in figure 3.23, then the TM_{10} and TM_{01} modes create respectively the linearly polarized Electric Fields equated in 3.15 and 3.16.

$$E_y = c \frac{sin(\frac{\pi}{L}y)}{k^2(1 - \frac{j}{Q}) - k_y^2} \tag{3.15}$$
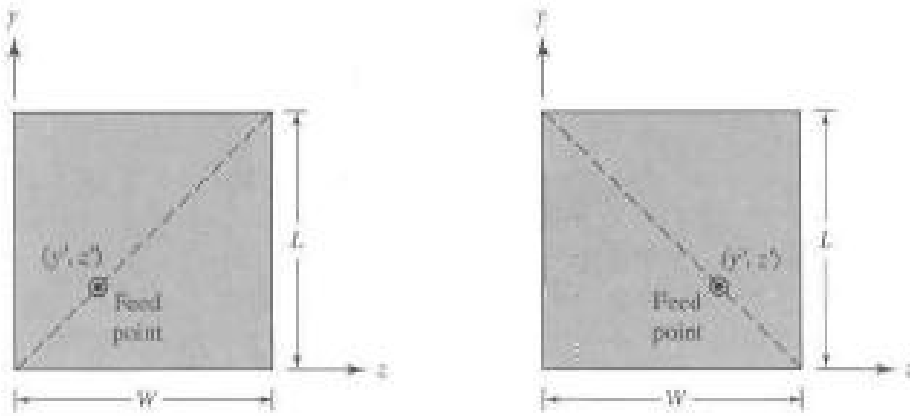
Figure 3.23: Diagonal Single-Feed Scheme[1]

$$E_z = c \frac{sin(\frac{\pi}{L}z)}{k^2(1 - \frac{j}{Q}) - k_z^2} \tag{3.16}$$

Q is the Quality Factor, $k_y = \frac{\pi}{L}$ and $k_z = \frac{\pi}{W}$ and k is the wavenumber at the central frequency f_0. Taking into account all of these equations, it's then possible to conclude that in order to create Circular Polarization, it's necessary to follow the condition presented in 3.17.

$$L = W(1 + \frac{1}{Q}) \tag{3.17}$$

The feeding point(y', z'), should be adjusted along the diagonal for the purpose of obtaining the Input Impedance as wished.

One alternative but similar way, used to create Circular Polarization without the need for a specific feeding point location is described using equation 3.18. In this equation $A = \frac{cos(\pi\frac{y'}{L})}{cos(\pi\frac{z'}{W})}$.

$$L = W(1 + \frac{A + \frac{1}{A}}{2Q_t}) \tag{3.18}$$

A different alternative to the two previously stated methods, that reaches an almost Circular Polarization, is next presented. It consists on using a square Patch with a slot whose dimensions are given by 3.19 and 3.20, as shown in figure 3.24. In this figure, the scheme on the left represents Left Hand Circular Polarization while the one on the right represents Right Hand Circular Polarization.

$$c = \frac{L}{2.72} = \frac{W}{2.72} \tag{3.19}$$

$$d = \frac{c}{10} = \frac{L}{27.2} = \frac{W}{27.2} \qquad (3.20)$$
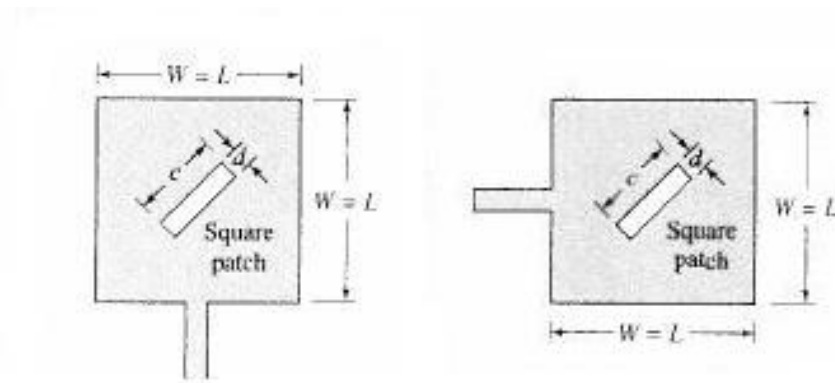
Figure 3.24: Creation of Circular Polarization by cutting slots in the Patch [1]

Finally, one last way to obtain Circular Polarization, and possibly one of the most commonly used is shown in figure 3.25. The Patch must be square and two of its opposite corners must be deleted. Moreover, the sense of the Polarization is determined by the relative position of the feed point to the deleted corners . In the presented figure the Polarization is Right Hand. If the Patch is rotated on itself 90º while keeping the feed point in the previous position, it's then possible to obtain Left Hand Circular Polarization. Finally it should be pointed out that, taking the case presented in figure 3.25 as reference, the *y* coordinate can be varied in order to obtain an Input Impedance match.
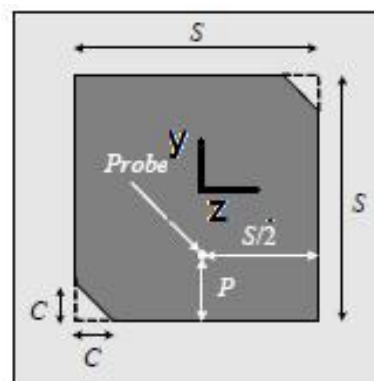
Figure 3.25: Trimmed Corners Microstrip Patch Antenna [14]

3.4   Circular Polarized Antenna Arrays

There are several reports of Circular Polarized Antenna Arrays in literature. Most of these are related in some way to global position, mobile, or satellite communication systems. In this section some examples of Circular Polarized Antenna Arrays are presented. They are the result of some literature research followed by a selection of those that seemed more interesting to the scope of this thesis. Moreover, Circular Polarized Antenna Arrays whose goal is to reach an Isotropic Radiation Pattern are of particular interest. However, limited results were reached as this seems to be a slowly progressing field of research. Due to amongst other things, its conformal characteristic, the most recently reported antenna arrays use as single elements Microstrip Patch Antennas.

In [17] a linear eight element Square Microstrip Patch Array operating in the L band is presented (see figure   3.26). The purpose of this array is to work in a wind profiling radar, being that this kind of radar generally measures wind direction and speed. Unlike what is the main objective of this thesis, for this application a narrow beam is necessary. A square patch was chosen in order to implement Circular Polarization. The method used was based on a proper placement of the feed. The design equations used were the Transmission Line typical ones, i.e.   3.1 and   3.2. This way, a Patch antenna with the next presented parameters was created: $a = 7.6cm$, $h = 3.175mm$ and $\varepsilon_r = 2.2$. By equating the Beam Width for a linear array, as a function of the antenna parameters, the main objective was obtained successfully, and so the basic design equations served their purpose.
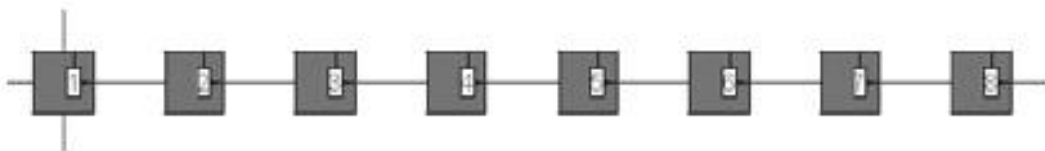

Figure 3.26: L band 8X1 Microstrip Patch array with 9^0 beam width [17]

Another array is presented in [18]. This is a Left Hand Circularly Polarized low cost Patch Array Antenna, whose aim is to provide the best axial ratio bandwidth. It's projected to work at $60GHz$ as it's intended for ultra-high speed short range wireless communications. The array is composed by square Patch with two opposite deleted corners, in order to achieve Circular Polarization. With the aim of achieving the best Polarization purity, an aperture coupled feeding scheme was used. Also, a sequential feeding array was utilized, which according to the authors implies a bigger axial ratio bandwidth. In this array, the elements are relatively rotated to each other by 90°, being that they are also fed with a relative phase difference with the same value as their physical relative rotation. In figure   3.27, the feeding scheme as well as the sub antennas built are presented. These

are obviously very small(in the order of hundreds of μm) due to the big frequency of operation.

Figure 3.27: 60GHz Square Patch Antenna Array and its Feeding Network [18]

The practical measurements show that this antenna has a 3 dB Axial Ratio Bandwidth of 11.25% with 10 dB return loss Bandwidth of 17%. This way the objectives initially proposed were achieved. The research conducted in this paper is relevant because not only it presents an implemented Circularly Polarized Antenna but also it gives some insight about the importance of the feeding scheme for the array functioning. Next, two cases of Circularly Polarized Antenna arrays whose objective was to achieve an Isotropic Radiation Pattern are presented. Both of the antennas presented were designed for cylindrical space vehicles. Unfortunately I was unable to find antenna arrays mounted on a cubic structure, as that would be more suitable for the scope of this thesis. This last remark may be an indicator that this is a specific field, still undeveloped.

In [19] a 2.25GHz Microstrip Antenna Array mounted on a cylindrical surface was developed for a Brazilian sounding rocket. The authors used a CAD tool named Cylindrical, in order to understand what was the minimum amount of sub antennas needed to achieve Isotropy. This previously stated CAD tool applies the cavity model to nearly square radiator Patch Antennas conformed on a cylindrical surface. As was said before in this thesis, in the case of space vehicles or satellites, the need for an Isotropic Radiation Pattern, comes when one wants to keep the telemetry communication reliable. In order to test the CAD program, the authors first built a single antenna using a substrate with the following properties: $h = 3.048mm$, $\varepsilon_r = 2.55$ and $\delta_{subs} = 0.0022$. An image of this antenna mounted on the rocket with a 0.25m radius can be seen in 3.28.

Because this antenna parameters were really close to what was expected, the authors proceeded to build the array. In order to achieve isotropy the sub antennas constituents of the array were disposed uniformly in a circle, driven by a current with the same amplitude and phase. For diverse reasons the authors decided to use 24 sub antennas, grouping them in three eight element sub arrays. In figure 3.29 the computed nearly Isotropic Radiation Pattern for the vertical plane is presented.
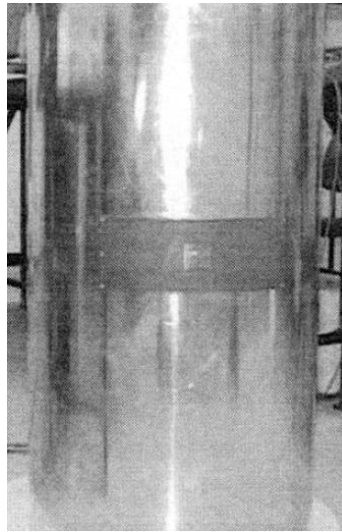
Figure 3.28: A 2.25*GHz* Nearly Square Patch Antenna mounted on a 0.25*m* radius cylindrical surface [19]
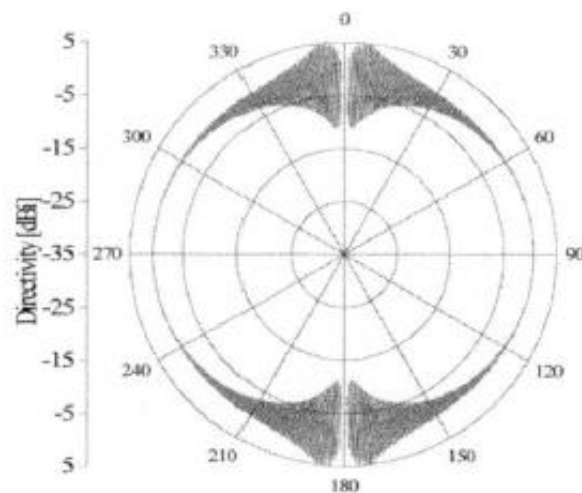
Figure 3.29: 24 Element Circular Array Computed Nearly Isotropic Radiation Pattern(vertical plane) [19]

Another work regarding the same area as the previous one is presented in [20]. Here, a circle of crossed slot radiators is studied. These slots are excited by two orthogonal TE modes in phase quadrature. They are driven by a current with a varying phase. This causes the Radiation Pattern to have a null at $\theta = 180^o$, being practically constant everywhere else. For better understanding of what has been said so far, there is a graphical representation in 3.30.

In [29], [30] a theoretical proof that a Circularly Polarized Isotropic Radiator is not achievable in practice is given. Quoting [20] "Either a -3 dB minimum, or less, distributed
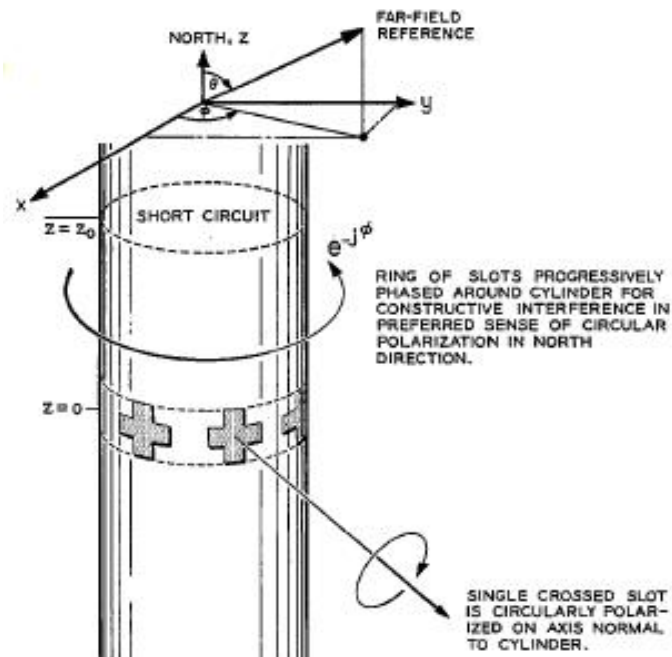
Figure 3.30: Slotted Ring Antenna Array Scheme [20]

over a finite portion of the sphere, or a zero at, at least, one point is required.". After deriving all the needed theory, the authors concluded that eight radiators were required. In figure 3.31 the Radiation Pattern for $\phi = 0^o$ is presented. As can be seen, it approximates Isotropy. In fact, experimental results showed that a gain bigger than $-3dB$ is maintained for $-168^o \leq \theta < 168^o$. As predicted there is a null in the south pole. However these are very good results, especially taking into account that the predicted Radiation Pattern was very close to what was obtained experimentally.

The themes here developed were the ones considered particularly important for this thesis. First, a brief revision of GPS was made, particularly concerning the importance of an Isotropic Radiation Pattern in the context of the Vorsat Project. After this, the Vorsat Project was quickly introduced, followed by a revision of some antennas used in small satellites. Particular relevance was given to Microstrip Patch Antennas since this seems to be the most proper kind of antenna for this kind of application. Next, some theory concerning Microstrip Patch Antennas and specifically rectangular ones was described. Also methods for Circular Polarization creation in this kind of antenna were researched. Finally some examples of Circularly Polarized Antenna Arrays were presented. Few of these were specifically conceived in order to achieve a near Isotropic Radiation Pattern.

With this in mind, one can conclude that this area of expertise is still in development as there aren't many examples of this kind of array.
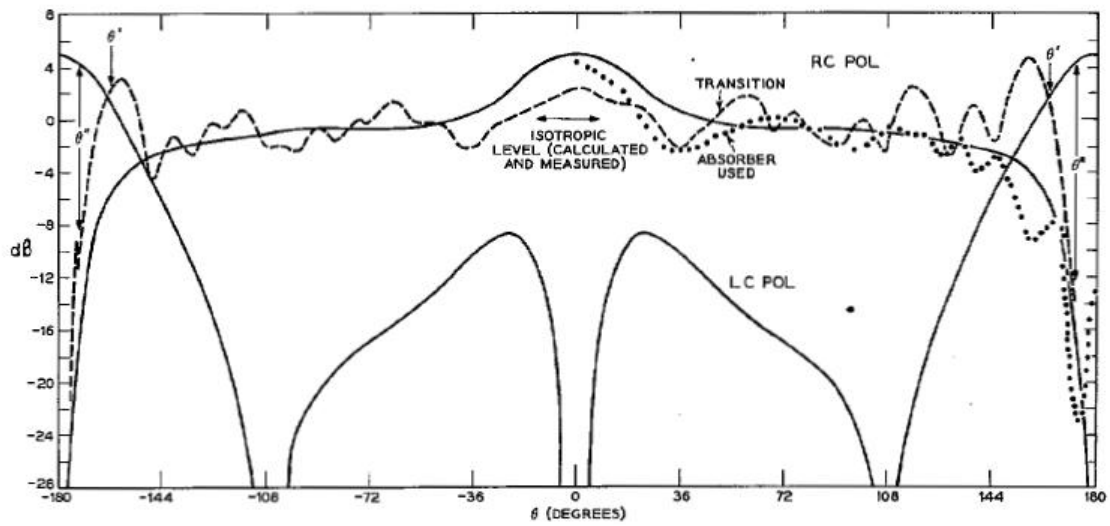
Figure 3.31: Near Isotropic Antenna Array Radiation Pattern for $\phi = 0^\circ$ [20]

Chapter 4

Design of the Array's Radiating Elements

In this chapter all the work related to the design and development of the sub antennas that constitute the array is presented. This includes, not only the choice of the sub antenna to be designed, but also the theory and equations behind this design.

4.1 Choosing the Antenna to Design

In chapter 3, several parameters considered important for the selection and design of Small Satellite Antennas were presented. As this is a small budget project and taking into account that one of the particular objectives of this thesis is to build a prototype of the Vorsat GPS Antenna, some major factors considered the most relevant ones were established. With this in mind, some of the constraints next presented are related to the GPS, while others are related to the context of the project itself.

1 The resonant frequency should be the central L1 band one, i.e. $1.57542 GHz$.

2 The Polarization should be Circular with an acceptable Axial Ratio.

3 The Bandwidth should be approximately 0.13% (1576.42 MHz-1574.42 MHz).

4 The antenna should be as small as possible, conformal and robust.

5 The costs associated to the manufacturing of each sub antenna that constitute the array must be relatively low, preferably using resources already available in the faculty.

As explained earlier in the Literature Review, the GPS operates at essentially two sub bands named L1 and L2, being that for civilian purposes only L1 is used, and so this antenna will be a single frequency band one. According to [13], a Bandwidth of approximately 0.13% should be considered for GPS applications. About the physical aspects of the antenna, lots of tests must be made in order to see if it performs as planned in the harsh low orbit environment. However, taking into account that the end product of this thesis is just a prototype, whose objective is to study a Radiation Pattern, such performance tests will not be considered. Another important issue for this project's communication system is related to the fact that, per face, three other antennas are needed for other purposes. However there are only six sides with approximately $100cm^2$ each where these can be distributed. These other three antennas will operate at nearly $2GHz$. Moreover, there will be the need for Solar Panels to be placed on the satellite's surface, in order for it to get some energy. These also occupy space but some integrated solutions grouping Microstrip Patch Antennas with Solar Panels have been reported in [31]. Also in [32] a similar solution is presented, in which the Patch is replaced by a special solar cell. As has happened before, the lack of space on the CubeSat's faces will not be considered a determinant issue in this prototype antenna design, since a variety of simple methods exist to solve this problem. The most common and already mentioned one, consists of using a substrate with a bigger Relative Permittivity. Another more complex option is proposed in [33]. Here the antenna miniaturization is achieved in about 36%, by cutting four small rectangles in the square Patch. Due to the importance of the last item presented in the previous table it was decided that taking into account the scope of this thesis and the availability of resources in the faculty's workshop, particularly when it comes to PCB's manufacturing, the best way to comply with the deadlines imposed was to use as sub antennas, Microstrip Patch Antennas with a FR-4 substrate. At this point it's important to explicitly state that the faces of the Cubesat will be made of this substrate material. This wasn't obviously the only fact that contributed to this decision. Also the availability of theoretical and practical reports related to the use of this kind of antenna in GPS communication, and the fact that these antennas have many characteristics that fit perfectly on what is desired for this array, made this kind of antenna a very desirable one. Finally another issue that must be addressed here is related to Circular Polarization. It was already mentioned in the previous chapters that GPS communication requires Right Hand Circular Polarization. One of the parameters of this kind of Polarization, to be taken into account is the Axial Ratio. In most of the literature reviewed while researching for this thesis I found out that a good Axial Ratio is one that doesn't exceed $3dB$. Also, the method to implement Circular Polarization in Microstrip Patch Antennas must be chosen. Based on the literature review presented in chapter 3, with the experience reported by the examples given in the various papers, the Trimmed Corners Square Patch Antenna seems to be a good option. This method only requires one feed, whose position can be adjusted for Input Impedance

matching. Also, the Circular Polarization performance is not so susceptible to the feed position, as it happens in other single feed methods. The feeding method chosen between the four previously mentioned was the Coaxial Line one. This method seems to satisfy the necessary demands, being that, due to the cubic structure inherent to the antenna array spatial disposition, this appears to be the most suitable one. To sum up, table 4.1 presents the main characteristics, as they were previously discussed, of the sub antenna to be designed.

Table 4.1: Resume of the Main Characteristics of the sub antenna

Parameters	Characteristics
Substrate	FR-4
ε_r	4.4
Thickness(m)	$1.6 * 10^-3$
Polarization	Right Hand Circular
Axial Ratio	$< 3dB$
Resonant Frequency(GHz)	1.57542
Bandwidth	$\approx 0.13\%$
Patch Shape	Trimmed Corners Square
Feeding Method	Coaxial Line
Input Impedance Matching	50Ω

4.2 Design of the Trimmed Corners Square Microstrip Patch Antenna

Due to reasons related to the complexity of the electromagnetic analysis of this kind of antenna functioning, the design process is usually divided into two steps. In the first step Analytical Methods based on the previously mentioned analysis theories are employed. These serve as a basis to the next step, which is to use Full Wave Analysis Method. This way better results are provided regarding the behaviour of the proposed antenna. The software available for this purpose at the Faculty of Engineering of Porto is named HFSS.

4.2.1 Design of the Square Microstrip Patch Antenna

In this section, the analytical methods employed in order to achieve a first draft of the desired antenna are documented. Some of the equations next presented are described in [16] while others have been already referred in chapter 3. The method followed here is mostly based in the Transmission Line Model. It was also used in [34], for exactly the same purpose, with good results. Just to complement, in this last mentioned PHD thesis,

the author writes a MathCad program for analytical design and Input Impedance evaluation of Trimmed Corners Square Microstrip Patch Antenna based on the Segmentation Method.

According to [1] a good estimation of the Patch Width is given by equation 4.1.

$$W = \frac{v_0}{2f_r}\sqrt{\frac{2}{\varepsilon_r + 1}} \tag{4.1}$$

This estimation can now be utilized to compute ε_{reff} by using the already presented equation 3.1. Having these two parameters, equation 3.2 is then used to take into account the Fringing effect. Finally, the Patch length can be calculated using equation 4.2.

$$L = \frac{v_0}{2f_r\sqrt{\varepsilon_{reff}}} - 2\triangle l \tag{4.2}$$

With a more accurate value for the Patch Length, and taking in consideration that this is a square Patch, the side of the square is set to L, i.e. $a = L$. Next, the value of the Quality Factor Q must be calculated because it will be very useful further in this chapter. To do so, it's first necessary to calculate the Conductance of a single slot G_1, and of another that simulates the mutual effects between the two slots of the Transmission Line Model G_{12}. Despite the value given by equation 3.5, using the Cavity Model, one can obtain a more accurate value for this parameter through equation 4.3. Here $k_0 = 2\pi f_0\sqrt{(\varepsilon_0\mu_0)}$ is the vacuum wavenumber and θ is the elevation angle.

$$G_1 = \frac{1}{120\pi^2}\int_0^\pi (\frac{sin(\frac{k_0W}{2}cos(\theta))}{cos(\theta)})^2 sin^3(\theta)d\theta \tag{4.3}$$

With G_1 calculated, G_{12} is given by equation 4.4 as presented in [1]. J_0 is the Bessel function, order zero of the first kind.

$$G_{12} = G_1 J_0(k_0 L sin(\theta)) \tag{4.4}$$

With both Conductances calculated, it's now possible to estimate Q. This parameter can be expressed using several Quality Factors, associated to the several losses inherent to the kind of antenna here under analysis. This can be seen in equation 4.5. Q_d is the Quality Factor that has to due with the dielectric losses, Q_c is associated to the conductor losses and Q_r is the most relevant one because it is related to the radiated power. It should be pointed out, that one source of losses was here neglected, i.e. the power loss associated to Surface Waves.

$$Q = (Q_d^{-1} + Q_c^{-1} + Q_r^{-1})^{-1} \tag{4.5}$$

Q_d and Q_c can be calculated according to equations 4.6 and 4.7, respectively.

$$Q_d = (\delta_{subs})^{-1} \tag{4.6}$$

$$Q_c = h\sqrt{\pi f_0 \mu_0 \sigma} \tag{4.7}$$

In this case, σ is the metal conductivity of the Patch, which for cooper is approximately $5.9610^7 Sm^{-1}$. For FR-4 and operating in the L1 band, δ_{subs} is about 1.610^-2. μ_0 is the vacuum permeability. According to [34] Q_r can be efficiently computed using 4.8. Z_0 is the Characteristic Impedance of a Microstrip Line and is given by $Z_0 = \frac{120\pi}{\sqrt{\varepsilon_{reff}}(\frac{a}{h}+1.393+0.667\ln(\frac{a}{h}+1.444))}$.

$$Q_r = \frac{\pi}{4Z_0(G_1 + G_{12})} \tag{4.8}$$

Finally, according to [16] some general formulas can be applied to estimate the Radiation Efficiency and the Bandwidth. In order to calculate the Radiation Efficiency e_r estimate, one must first calculate the Radiated Power P_r and the Surface Wave Power P_{sur}, being that an approximate value of both of them can be obtained using 4.9. Here, $x_0 = 1 + \frac{1}{2}(\frac{\varepsilon_r - 1}{\varepsilon_r}k_0h)^2$, $k_0 = 2\pi f_0\sqrt{\varepsilon_0\mu_0}$.

$$
\begin{aligned}
P_r &= 40k_0^2(k_0h)^2(1 - (\varepsilon_r)^{-1} + \frac{2}{5\varepsilon_r^2}) \\
P_{sur} &= 30\pi k_0^2 \frac{\varepsilon_r(x_0^2 - 1)}{\varepsilon_r\left[\left(\sqrt{x_0^2 - 1}\right)^{-1} + \frac{\sqrt{x_0^2-1}}{\varepsilon_r - x_0^2}\right] + k_0h\left[1 + \frac{\varepsilon_r^2(x_0^2-1)}{\varepsilon_r - x_0^2}\right]}
\end{aligned}
\tag{4.9}
$$

With this in mind, the Radiation Efficiency is then computed by $e_r = \frac{P_r}{P_r + P_{sur}}$. An error bigger than 5% is not expected for a square Patch, as long as $h\sqrt{\varepsilon_r} < \frac{\lambda_0}{8}$.

Finally one can now calculate the estimate for the Bandwidth using equation 4.10. Some approximations were made due to the square shape of the Patch, i.e. $p \simeq 1$, $\frac{W}{L} = 1$ e $q = 1 - \varepsilon_r^{-1} + \frac{2}{5\varepsilon_r^2}$.

$$BW = \frac{16}{3\sqrt{2}}\frac{p}{e_r}\frac{1}{\varepsilon_r}\frac{h}{\lambda_0}\frac{W}{L}q \tag{4.10}$$

With equations for almost all the important parameters of the antenna presented, there's still a very important one that wasn't yet mentioned, i.e. the Input Impedance. In fact, as the antenna so far projected is only a square Patch one, the Input Impedance could be accurately estimated by applying the Parallel RLC Network Model, derived from the Cavity Model assumptions in [35]. In this model, used for Input Impedance computation purposes, each mode is represented by a Parallel RLC circuit. In the Circular Polarization case, usually modes (1,0) and (0,1) are excited. This way, by considering these two plus

the (0,0) one, a very good estimation of the Input Impedance could be made. However, as the Patch will in fact have two trimmed corners, the previous mentioned method can no longer be applied. For such case, the Segmentation Method is the proper one. This is fully explained and derived in [34]. This derivation is not an easy one. Taking all of this into account, I decided that it would be better to achieve Input Impedance matching on a trial and error approach using HFSS.

Table 4.2: Analytically derived Antenna Main Characteristics

Parameters	Value
Square Patch Side Length	$4.5cm$
Quality Factor	37.4301
Radiation Efficiency	93.24%
Bandwidth	0.61%

With the basic parameters of the desired antenna calculated using the previously reported formulas and summarized on table 4.2, it's now important to explore the method to turn this antenna into a Right Hand Circular Polarized one. A quick note is made to the fact that the predicted Bandwidth complies with the GPS standard.

4.2.2 Right Hand Circular Polarization Implementation

With an estimative of the desired antenna parameters already obtained, it's now important to select and develop a method to implement Right Hand Circular Polarization in this antenna. Some methods for this purpose were already described in the Literature Review, being that two of these appear to be the most popular ones. The first has its algorithm deeply described in [36]. It briefly consists on placing the feed in a specific point on the Patch. The second, that was the chosen one to be implemented on this thesis for previously stated reasons, is fully described in [16]. Once again, as was already mentioned, it consists on trimming two opposite corners of a square Microstrip Patch Antenna.

Next the theoretical basis of this last method is presented, step by step, according to the already mentioned source. The idea is to reach some relation that will allow us to calculate the area of the Patch that needs to be cut out.

In general terms and as has been described in more detail in the previous chapter, the idea is to place the feed point in a certain position in respect to the trimmed corners of the Patch, so that two orthogonal modes with the same amplitude but $\frac{\pi}{2}$ phase lagged, are created. In figure 4.1 one can observe a general scheme of the antenna that is the result of this method's application.

The cuts performed on the Patch corners will result in the modification of the eigenvalues of the fields of the modes of the cavity that the antenna constitutes. These can be determined from equation 4.11. In this equation, ϕ' is the new mode, k' is the new eigenvalue, S is the Patch total area and ΔS is the area of the perturbation.
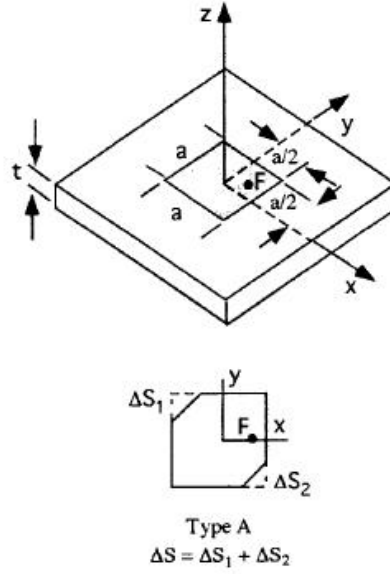
Figure 4.1: General Scheme of the antenna to be implemented by this method[16]

$$k'^2 = \frac{\int_{S+\Delta S} \nabla \phi' \cdot \nabla \phi' dS}{\int_{S+\Delta S} \nabla \phi'^2 dS} \tag{4.11}$$

ϕ' can be equated as $\phi' = P\phi_a + Q\phi_b$, i.e. as a function of the degenerate modes of the square Patch antenna. This way, by substituting the previously stated relation of ϕ' in equation 4.11 and by performing some manipulations (described in detail in the book already stated), one obtains equation 4.12 and the determinant 4.13.

$$\frac{\partial U(P,Q)}{\partial P} - k'^2 \frac{\partial V(P,Q)}{\partial P} = 0$$
$$\frac{\partial U(P,Q)}{\partial Q} - k'^2 \frac{\partial V(P,Q)}{\partial Q} = 0 \tag{4.12}$$

$$det \begin{bmatrix} k^2 + q_1 - k'^2(1+p_1) & q_{12} - k'^2 p_{12} \\ q_{12} - k'^2 p_{12} & k^2 + q_2 - k'^2(1+p_1) \end{bmatrix} = 0 \tag{4.13}$$

For a square Patch, it's known that, and following the same axis configuration as presented in figure 4.1, the equations of the degenerate modes TM_{010} e TM_{100} are given by 4.14. In this equation $V_0 = \frac{\sqrt{2}}{a}$ and $k = \frac{\pi}{a}$ and $a = W = L$.

$$\phi_a = V_0 sin(kx)$$

$$\phi_b = V_0 sin(ky) \tag{4.14}$$

Using the equations so far described, one can reach equations 4.15.

$$q_1 = q_2 = q_{12} = 0$$
$$p_1 = p_2 = \frac{2\Delta S}{S}$$
$$p_{12} = \frac{-2\Delta S}{S} \tag{4.15}$$

Substituting 4.15 in 4.13, the new eigenvalues k'_a e k'_b related to the new modes ϕ_a e ϕ_b, are obtained. The relation between these is given by equations 4.16.

$$k'^2_a = k^2(1 + 4\frac{\Delta S}{S})^{-1}$$
$$k'^2_b = k^2 \tag{4.16}$$

Taking this into account it's understandable how do the two modes frequencies change as a function of the perturbation ΔS. These are stated in equations 4.17. Here f_{0r} is the resonant frequency of the antenna before the perturbation is done. As one can see the frequency shift occurs only for one of the modes. In this case that mode is TM_{100}.

$$f_a = f_{0r} + \Delta f'_a = f_{0r}(1 - 2\frac{\Delta S}{S})$$
$$f_b = f_{0r} + \Delta f'_b = f_{0r} \tag{4.17}$$

It is now possible to reach a relation for some parameters of the equations presented here, on which non relation had been reached before. These will be important in order to achieve an equivalent circuit that will allow the two previously stated modes to be analysed. This analysis will be used to impose some constraints for the Circular Polarization creation. These relations are stated in 4.18, in 4.19 and in 4.20. In equation 4.19, ϕ'_a and ϕ'_b are equations that refer to the new modes. In its derivation, the approximation $k'_a = k'_b = k$ was assumed. In equation 4.20, N'_a and N'_b correspond to the distribution of energy by the two modes, being that this is modelled here as the ratio of turns of a transformer.

$$P_a = -Q_a = \frac{1}{\sqrt{2}}$$

$$P_b = Q_b = \frac{1}{\sqrt{2}} \tag{4.18}$$

$$\phi_a' \approx \frac{V_0}{\sqrt{2}}(sin(kx) - sin(ky))\phi_b' \approx \frac{V_0}{\sqrt{2}}(sin(kx) + sin(ky)) \tag{4.19}$$

$$N_a' = \frac{\sqrt{S}}{a}(sin(kx) - sin(ky))N_b' = \frac{\sqrt{S}}{a}(sin(kx) + sin(ky)) \tag{4.20}$$

It's now possible to create the already mentioned electric equivalent circuit for the Patch, with the perturbation already being included. This circuit is presented in figure 4.2. In this figure, Y_a' and Y_b' represent the Input Admittances of the Patch for each mode. G_a' and G_b' represent various losses.
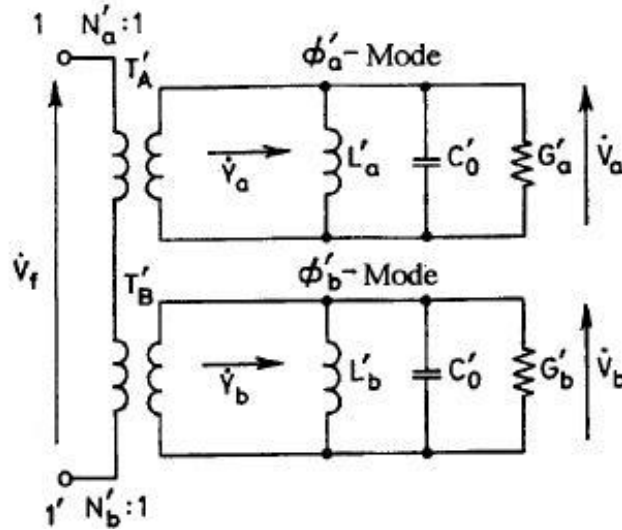

Figure 4.2: Equivalent Circuit for the antenna with the Perturbation included[16]

Taking this circuit into account, it's now possible to establish conditions for the creation of Circular Polarization, in order to obtain a closed end condition. To this end, we know that the ratio of the two ratios between the amplitudes of the two modes are given by equation 4.21. Q_0 is the Quality Factor of the Patch before any perturbation occurred. It's the same for both modes.

$$\frac{V_b}{V_a} = \frac{N_b'}{N_a'}\frac{Y_a'}{Y_b'} = \frac{N_b'}{N_a'}\frac{\frac{f_a}{Q_0} + j(f - \frac{f_a^2}{f})}{\frac{f_b}{Q_0} + j(f - \frac{f_b^2}{f})} \tag{4.21}$$

In order to create Circular Polarization it's known that the ratio of the two modes amplitudes has to follow $\frac{V_b}{V_a} = \pm j$. Therefore, if the ratio $\frac{N_b'}{N_a'}$ is equal to unity, then equation 4.22 can be derived.

$$\frac{V_b}{V_a} = \frac{\frac{f_a}{Q_0} + j(f - \frac{f_a^2}{f})}{\frac{f_b}{Q_0} + j(f - \frac{f_b^2}{f})} \tag{4.22}$$

From now on, one can reach a simple result through algebraic manipulation. Such result is stated in equation 4.23.

$$\left|\frac{\Delta S}{S}\right| = (2Q_0)^{-1} \tag{4.23}$$

In order for constraint $\frac{V_b}{V_a} = \pm j$ to be followed, it's still necessary, according to equation 4.20, that the feed position is placed along one of the two axis, either x or y, as shown in figure 4.1. In the Right Hand Circular Polarization case, the feed should be placed along the y axis. Thereafter, any change in this axis can be performed in order to obtain the desired input impedance, i.e. 50Ω.

Equation 4.23 was used to compute the area needed for the perturbation. The obtained value was $2.7101e - 005m^2$. This means that the side of the square to be subtracted to the patch is $5.2mm$.

With the initial design for the antenna all set, it's now possible to use HFSS to simulate, analyse and improve, the performance of the so far analytically designed antenna.

4.2.3 Simulation and Refinement of the Antenna Performance Using HFSS

In this section, the final steps towards the design of the sub antenna are described. Because HFSS offers a wide variety of options and has countless functionalities, the tutorial [37] was initially followed, since it provides the basic knowledge needed to operate this software, through practical examples. At this point some insight on the Vorsat exact dimensions must be given. After some study considering the size of the cubesat and taking into account its general specifications presented in [38], a general scheme with the exact measures needed for the faces of the cube was made and is now presented in figure 4.3. As one can observe, the faces have a slightly smaller area than what was initially said. This is due to construction details, mainly owing to the cube support structure.

Because the initial objective was just to see how the analytically designed antenna performed, it was placed on the center of a FR-4 substrate with the dimensions of a lateral face of the satellite. This can be seen in figure 4.4. It's important to state that the feed position, that can clearly be seen in the image presented, was, as said before, the result of a trial and error method, performed until the best Input Impedance for matching purposes was obtained.

The results obtained were surprisingly good. In fact, all the parameters seem to be well adjusted to what was wanted. In figures 4.5, 4.7, 4.6 these simulation results are
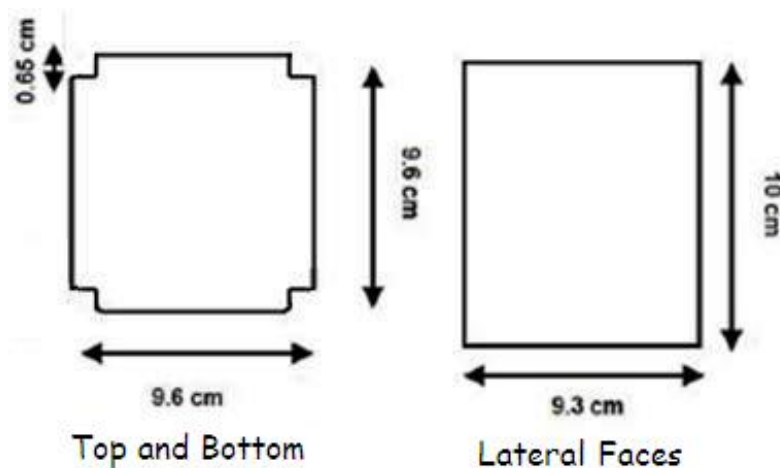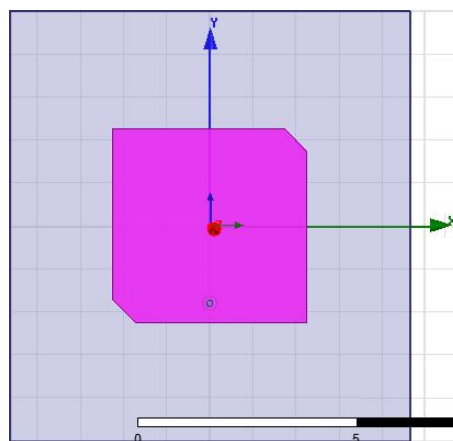
Figure 4.3: True Dimensions of the Vorsat's faces

Figure 4.4: Physical Model built on HFSS of the analytically conceived antenna

presented. The Input Return Loss($S11$) parameter reaches its minimum value of approximately $-18.5dB$ for a resonant frequency of $1.5750GHz$. This is a good result that shows that this is a good antenna for the intended frequency. The value obtained for the Axial Ratio is very good because it rounds $2.4dB$ (as was already mentioned less than $3dB$ is a good result). Finally the Input Impedance for the GPS L1 band center frequency is about $62.43 + j4.42\Omega$ which is a very acceptable. So far these results seem to prove that the analytical method used can be efficiently applied to the design of Trimmed Corners Square Patch antennas.

The next logical step was to try to arrange the antenna in a corner of the face of the cube, aimed at a better use of space. This has some implications because the area of substrate next to two sides of the patch is then radically smaller. This way, one could expect this to affect the Fringing fields. As predicted, some parameters suffered sever
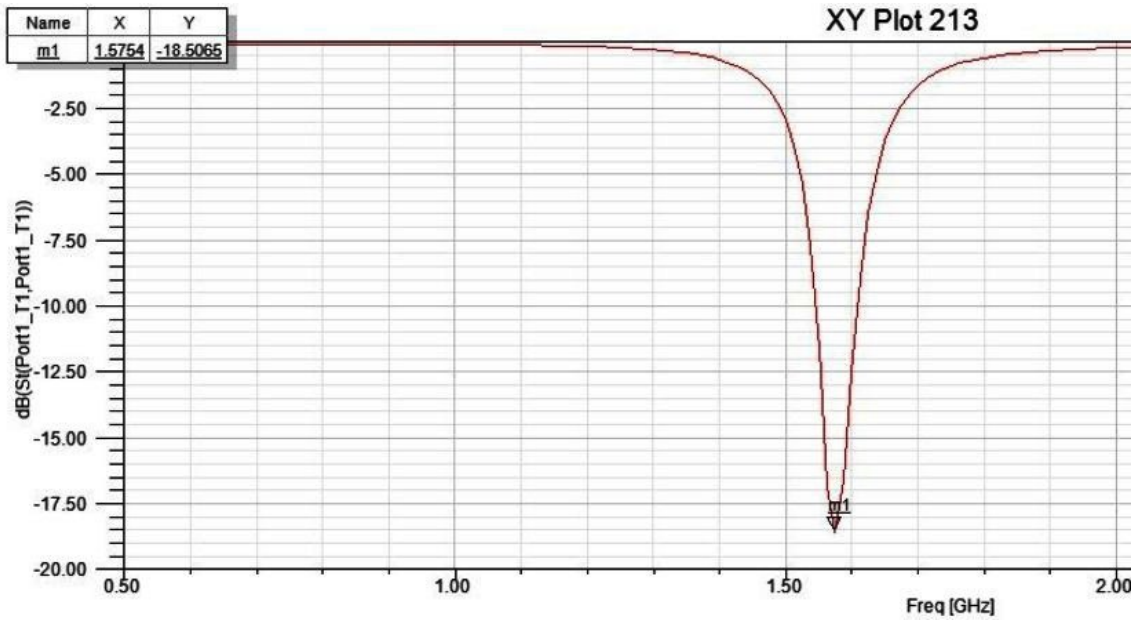
Figure 4.5: Results of the simulated analytically conceived antenna-S11
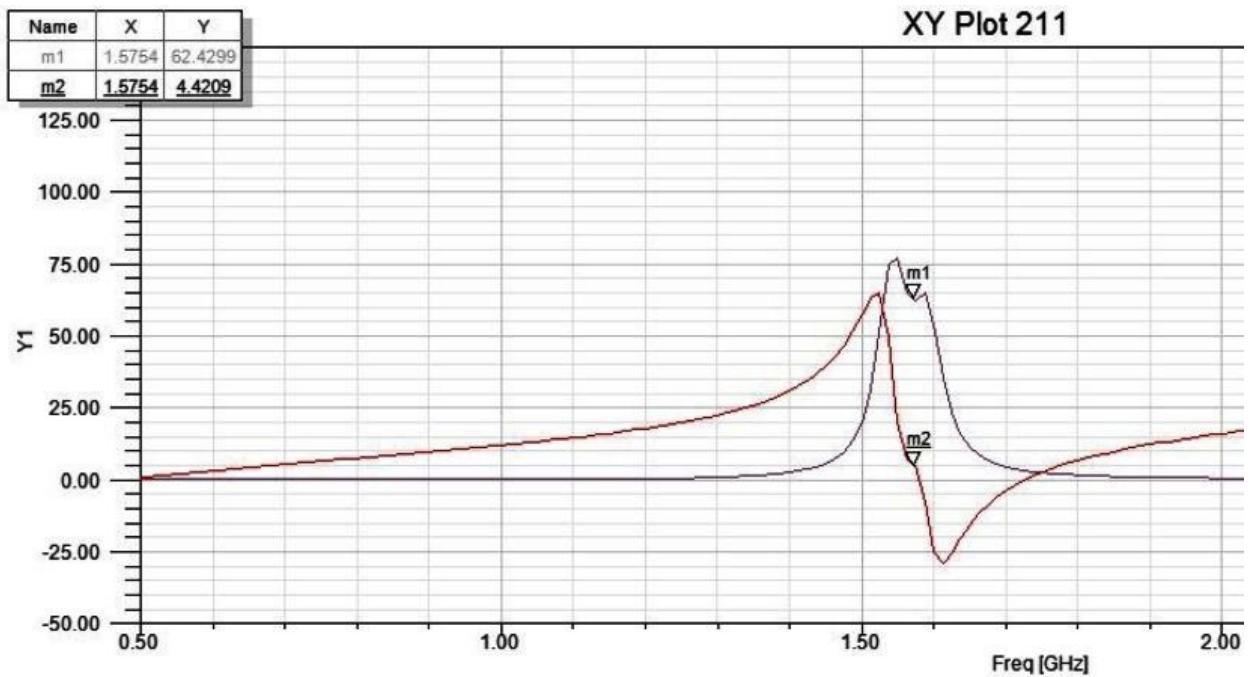
Figure 4.6: Results of the simulated analytically conceived antenna-Input Impedance. The real component is in grey while the imaginary is in red.

changes. In particular the Input Impedance and the Axial Ratio changed to unacceptable values. This fact led to a trial and error approach using simulation in order to modify this values. To do so, both the trimmed area and the feed position were continuously

Figure 4.7: Results of the simulated analytically conceived antenna-Axial Ratio. Two pattern cuts are represented, one in red for $\phi = 0^o$ and one in grey for $\phi = 90^o$.
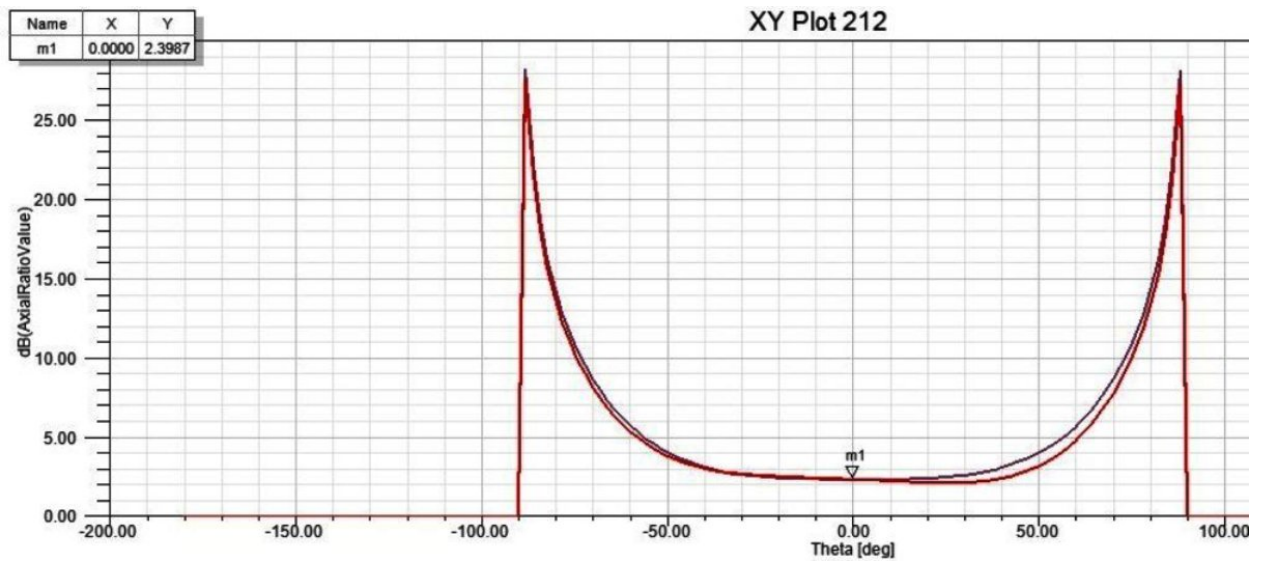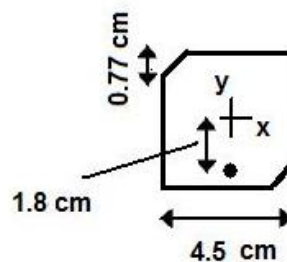
Figure 4.8: General Scheme of the newly developed Patch

modified until what appeared to be the best results possible. The new dimensions of the Patch are presented in a scheme in figure 4.8. As can be noticed, the length of the side of the square cut out from the Patch rose from $5.2mm$ to $7.7mm$. The S11 parameter, Input Impedance and Axial Ratio are presented in figures 4.9, 4.10 and 4.11. From the analysis of these results one can conclude that the $S11$ parameter is still good, although apparently, this antenna has its best behaviour at a slightly lower frequency value. Also, the Input Impedance achieved proper results for 50Ω matching, although the Reactance is now a bit higher. About the Axial Ratio, one can say that it was noticeably degraded as it now surpasses the $3dB$ limit value. However, after some consideration, it was decided that the value around $3.8dB$ is an acceptable one.

Finally, one last result was analysed just to confirm, what was already mentioned in the Literature Review. It's related to the shape of the antenna's gain. Such result is graphically presented in 4.12. As predicted the gain achieves its maximum in a direction

XY Plot 210

Name	X	Y
m1	1.5750	-19.9798

Figure 4.9: Some results of the simulated sub antenna on the right top corner of the substrate structure(satellite's face)-S11

XY Plot 209

Name	X	Y
m1	1.5750	9.9845
m2	1.5750	52.6958

Figure 4.10: Some results of the simulated sub antenna on the right top corner of the substrate structure(satellite's face)-Input Impedance. The real component is in grey while the imaginary is in red.

normal to the Patch. It should be noticed that during all of these simulations, the Ground Plan was considered to be infinite and so the antenna does not radiate past the $+/-90^{\circ}$ of elevation. In reality, this is not exactly true as Back Radiation usually exists. However as its value is usually very small, it was not taken into account here.
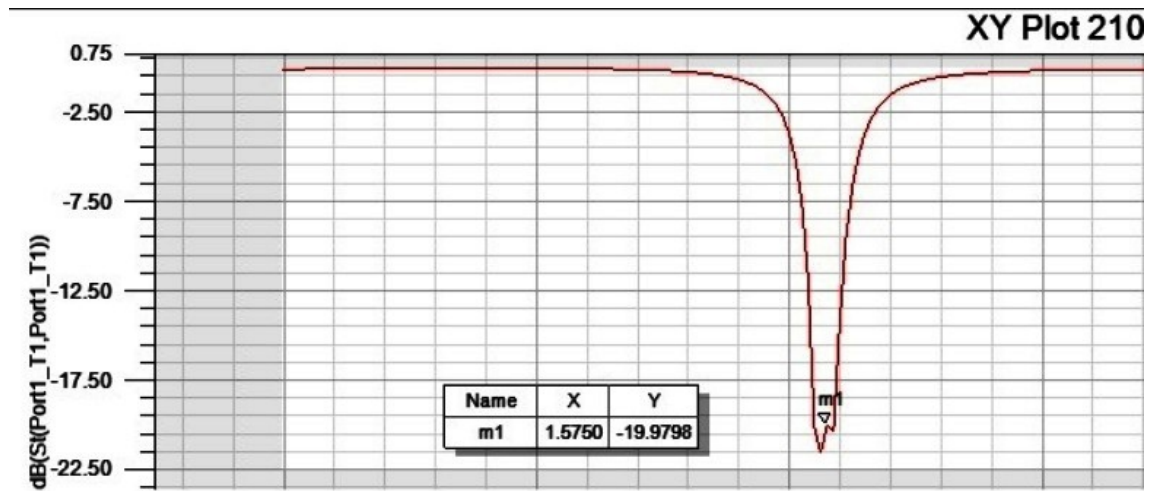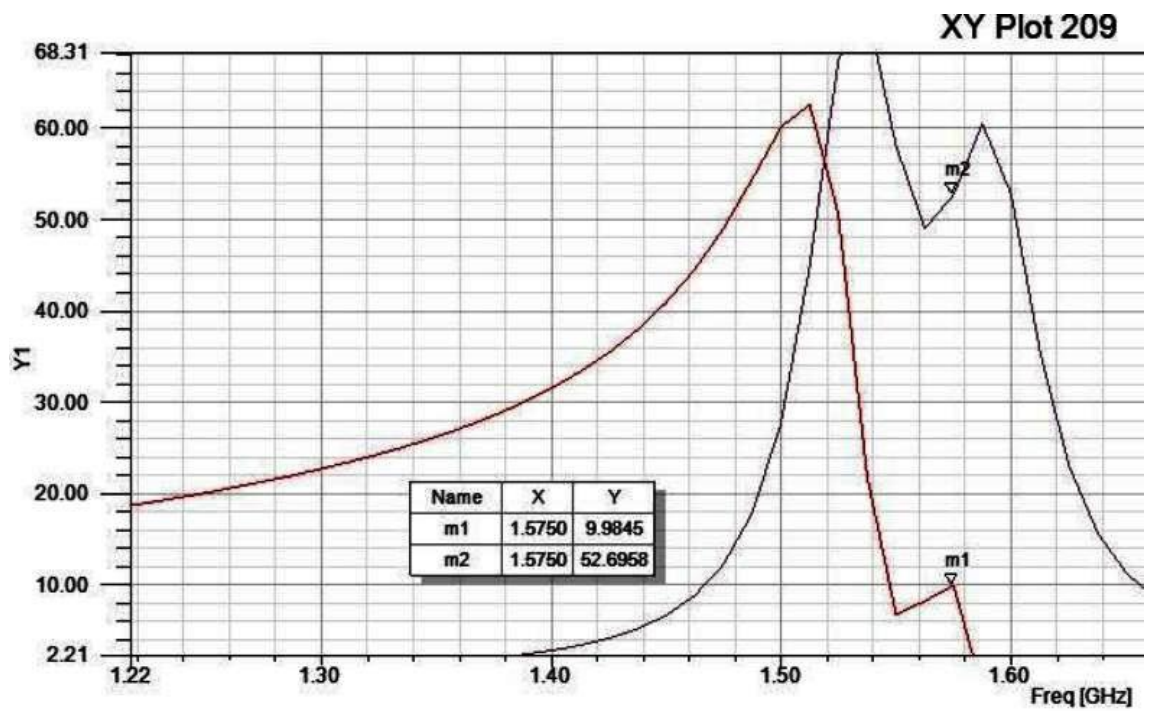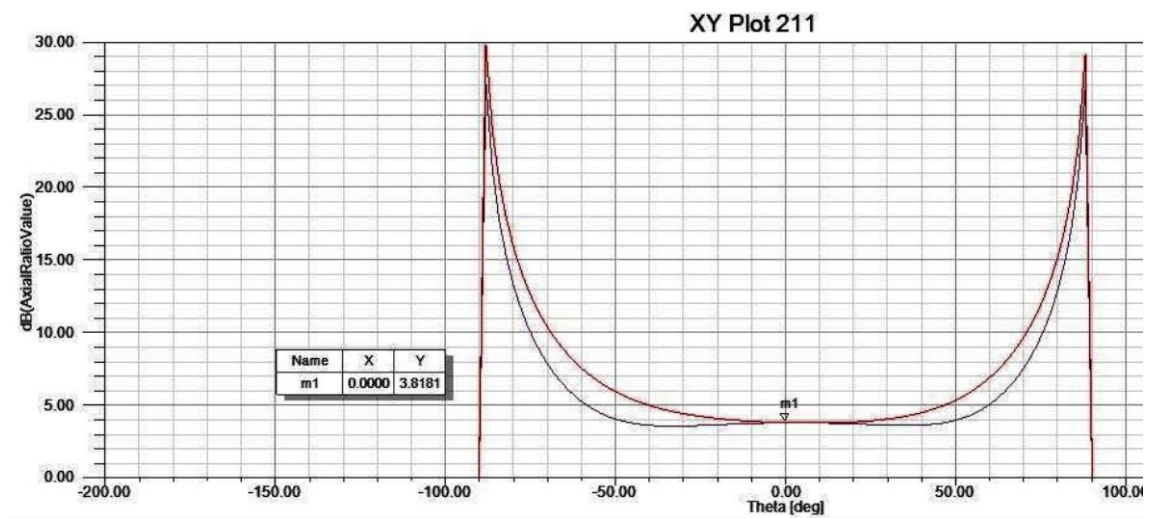
Figure 4.11: Some results of the simulated sub antenna on the right top corner of the substrate structure(satellite's face)-Axial Ratio. Two pattern cuts are represented, one in red for $\phi = 0^\circ$ and one in grey for $\phi = 90^\circ$.
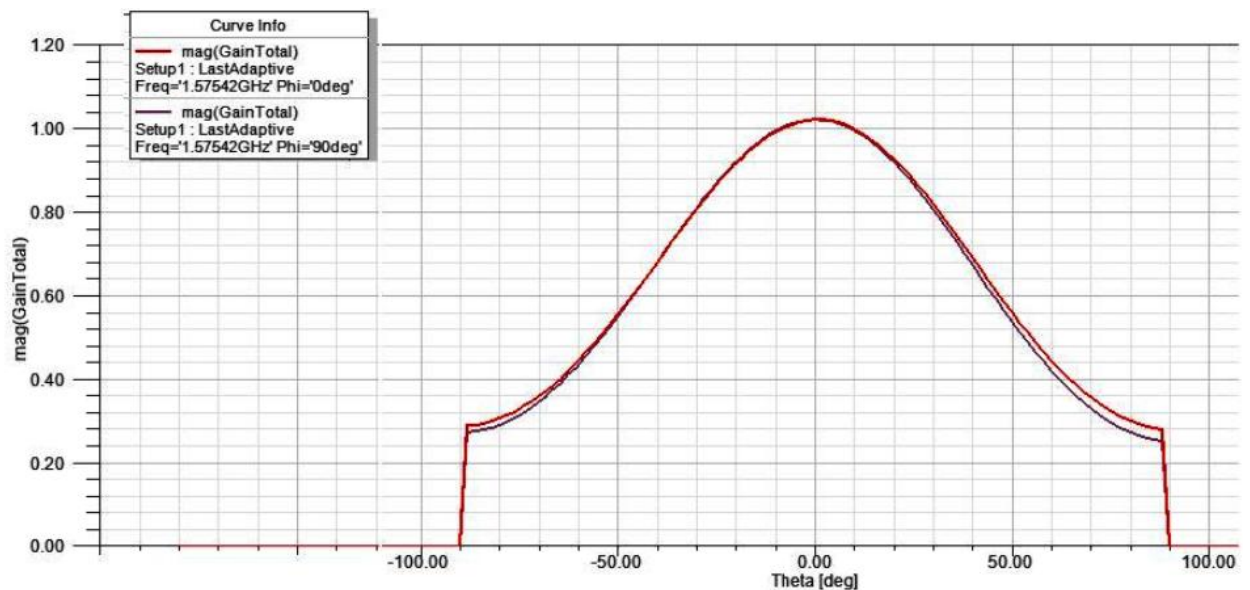
Figure 4.12: Gain of sub antenna designed. Two pattern cuts are represented, one in red for $\phi = 0^\circ$ and one in grey for $\phi = 90^\circ$.

In this chapter all the process that led to the design of the sub antenna that constitutes the array was presented in detail. It started off as an analytical process, leading afterwards to a trial and error one, with the help of a simulation software. The analytical process led to very good results, proving that the employed method fit what was necessary. The

need for the antenna to be placed in a corner, due to issues related to the use of space, made it necessary to make some changes to the initial structure of the Patch, in order to improve some of the antenna's parameters. The best result achieved was presented, and it's considered to be a good one. The most problematic parameter is the Axial Ratio, since it surpassed the initially desired $3dB$.

Chapter 5

Design of the Antenna Array

Since a sub antenna configuration now exists, it makes sense to proceed to an analysis of the array itself, whose final objective is to determine the array's characteristics, in order to obtain the desired Isotropic Radiation Pattern. Having said that, throughout this chapter, issues related to the analysis and design of this array will be discussed, with primary emphasis on the program developed for these purposes.

5.1   Array Structure and Desired Radiation Pattern

As it was mentioned before in this thesis, this array of Microstrip Patch Antennas is part of a GPS Receiver System, so that the Vorsat can locate itself when in orbit. Due to the small size of the satellite, and the need for other structures, e.g. other antennas and solar panels, to be put on the cube's faces, the spatial placement of the sub antennas that constitute this array is a very important matter. So, to sum up, two important values must be considered. The first one is related to the sub-antenna area, whose value is approximately $20.25 cm^2$. The second is related to the area of the cube's faces(see figure 4.3). The top and bottom faces have an area of about $92 cm^2$ while the lateral faces have one more square centimetre available. Taking all of these facts into account, a decision of using just one antenna per face, accounting to a total of 6 antennas, was seen as the right one. Of course it's also possible to use more than one antenna per face, by using smaller sub antennas than the one previously designed, as it may lead to a Radiation Pattern closer to isotropy. However for this prototype the previously stated option will be explored. In figure 5.1 a drawing of the Vorsat's faces is presented. Three smaller antennas and a bigger black one can be seen per face. This last one accounts for the GPS sub antennas that take part of the array here in discussion.

Figure 5.1: Vorsat's faces drawing [21]

With the basic array parameters defined, it's then logical that the next step consists on understanding how do the six sub antennas interact. In particular the biggest interest is related to the Radiation Pattern, since this is wanted as close as possible to isotropy ,so that the GPS reception is reliable. The fact that this interaction is not at all easy to analyse, in particular, due to the kind of polarization in question, makes it necessary to create a software capable of computing this interaction. Such software will be the subject of the next section of this thesis.

5.2 Array Simulation Software Development

In order to develop a software capable of simulating the interaction between the various antennas, Matlab was chosen. This software, in addition to widely distributed, it also allows easier handling of Matrices, for what it seemed to be the most suitable one. In figure 5.2 a GUI is presented. It was developed to make the array simulation software an easy one to use. Next some insight is given on how to interact and what are the functionalities of the developed software.

There are four variables of the array that one can use to obtain the intended Radiation Pattern. These are also the inputs to the developed array simulation software and are next presented.

1 The number of sub antennas that constitute the array.

2 The Cartesian spatial coordinates X, Y, Z (in meters) of the Patch center of the sub antennas.

3 The orientation in Spherical Coordinates (elevation and azimuth) of the vector normal to the Patch (direction of propagation of the wave emitted by the antenna), as well as the Initial Phase (rho_{ini}) of the Electric Field vector, normal to the direction of propagation. All these angles should be considered in degrees.
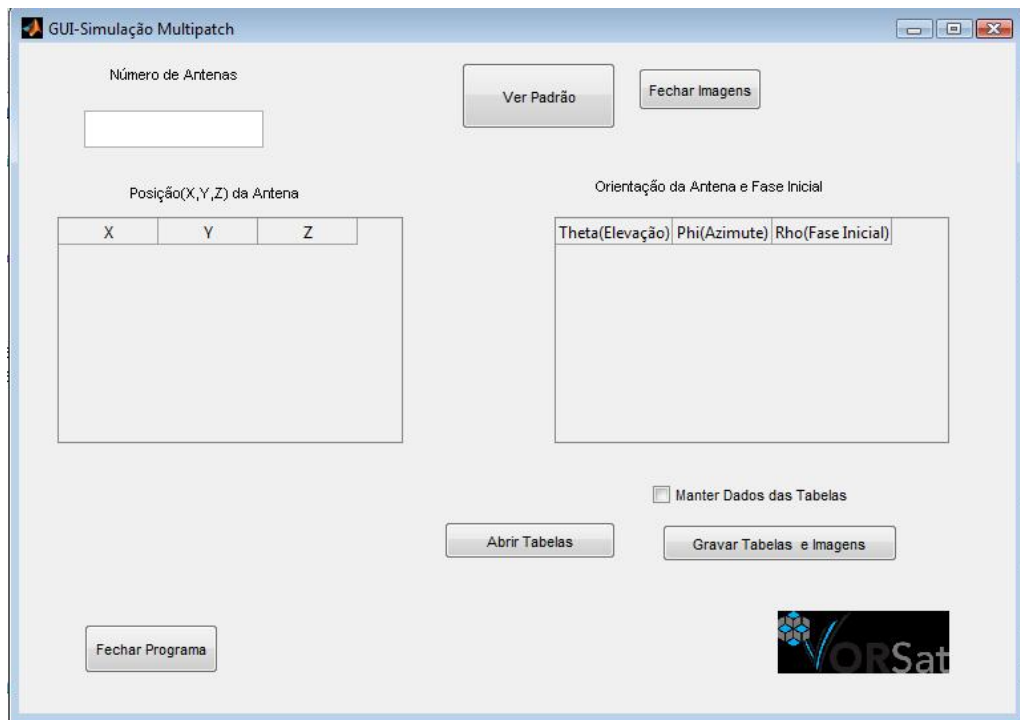
Figure 5.2: GUI

Before proceeding it's important to define a system of coordinate axes as is used in the developed software. Such a representation is presented in figure 5.3.
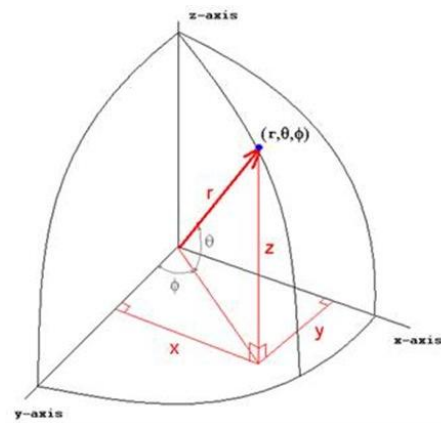
Figure 5.3: Graphical Representation of the Reference Coordinate Axes

There are a few functionalities that the already presented GUI provides. These are: Radiation Pattern View, Saving of the tables with the user input values and the respective images of the simulations, Opening of the Text Files where the inputs values had been saved. In the specific case of the great purpose of this program that is to View the Radiation Pattern, when one enables this feature, a new window with four processed images

appears. In fact, besides the Three Dimensional Surface Radiation Pattern Graphic, representing the Amount of Energy received by a Right Hand Circular Polarized antenna, it's also possible to observe the Patch antenna's positions on the Cubesat's faces,and again a 3D plot of the same Amount of Energy Left Hand Circular Polarized Antenna and also for a Right Hand one. As an example, in figure 5.4 the previously described images for just one Patch antenna, located on the center of one of the cube's faces with elevation, azimuth and Initial Phase equal to zero, are presented. On the top left corner one can see the 3D Surface Radiation Pattern graphic. To its right there is the already mentioned alternative representation of the same values. In the lower left corner there is the same measurement but for Left Hand Circular Polarization. Finally in the remaining picture, the position of the patch in the satellite is represented. Also one can see the vector normal to the Patch and the Initial Phase of the Electric Field Phasor, taking only into account the user's input.
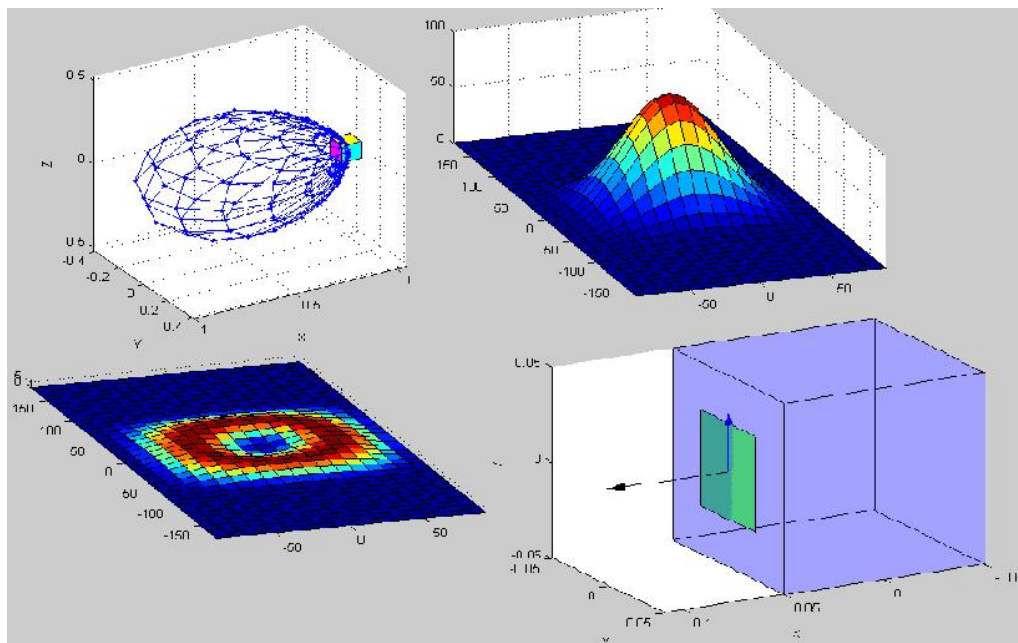
Figure 5.4: Images presented by the software for the Radiation Pattern analysis.

With the general outlines of the array simulation software clarified, it's now time to proceed to a brief explanation of how does the algorithm works. This consists in three iterative cycles, two of them perform a sweep of the whole space and the other one other for each sub antenna. Both in the elevation and in the azimuth, iterations of 10° are made. Besides this, the following unitary vectors are also defined:

1 One points in the direction of the observer, therefore varying with the iterations of the elevation and azimuth.

2 Two other with a phase difference of 90°, normal to the previously described one, representing the Vertical and the Horizontal Polarizations.

3 A unitary vector defined in the direction normal to the antenna, as set by the orientation (elevation and azimuth) inserted into the GUI by the user.

Using this last mentioned unitary vector and the one that points towards the observer, one can compute the angle of sight Δ_{angs}, and use it to calculate an approximate value of the Magnitude of the Electric Field , using equation 5.1. It should be pointed out that this equation is just an approximation of what one believes to model this magnitude. If the module of Δ_{angs} is bigger than 90°, then the magnitude is considered to be null, i.e. the Patch only radiates in the frontal direction.

$$mag = cos(\frac{\pi}{2}sin(\Delta_{angs}\frac{\pi}{180})) \tag{5.1}$$

It's now important to calculate the phase of the Electric Field Vector (ρ). This can be done through the sum of three components according to equation 5.2. ρ_{ini} is the user defined Initial Phase. It exists so that the Phase difference of the Electric Field wave of the sub antennas in relation to the other sub antennas is set. ρ_{pos} results from the projection of the antenna's position vector (X,Y,Z), defined as $\mathbf{P}$, in the direction of the observer unitary vector defined as $\widehat{\mathbf{O}}$, multiplied by $\frac{360}{\lambda}$ where λ is the wavelength at the L1 center resonant frequency, i.e 1.57542GHz. This can better be seen in equation 5.3. ρ_{pol} varies linearly, due to an iterative cycle, thus creating the rotation of the electric field derived from the type of polarization in question.

$$\rho = \rho_{ini} + \rho_{pos} + \rho_{pol} \tag{5.2}$$

$$\rho_{pos} = \frac{360}{\lambda}(\mathbf{P} \cdot \widehat{\mathbf{O}}) \tag{5.3}$$

Finally, the Electric Field Vector of each antenna is projected in the direction of the unitary vector corresponding to the Horizontal and Vertical orientations of the Polarizations. For each spatial point the Module and Phase of the resulting vectors for these two Polarizations (0° and 90°) are obtained. This way, there exist two markings, in Phase and Module, of the Electric Field that is being received. These constitute points of an Ellipse, and by using them one can calculate R_M and R_m which are respectively the major and minor axis of the Ellipse. These can be obtained by using the relations described in 5.4. Here, M_{00} is the already mentioned marking corresponding to 0° and M_{90} is the one corresponding to 90°.

$$\begin{aligned} \alpha &= abs(M_{00})^2 + abs(M_{90})^2 \\ \beta &= imag(M_{00} * conj(M_{90})) \end{aligned} \tag{5.4}$$

Now one can use α and β to calculate R_M and R_m. This can be done by using equation
5.5 if $(\frac{\alpha}{2})^2 - \beta^2 \geq 0$ or by using 5.6 otherwise. In both cases $R_m = \frac{\beta}{R_M}$.

$$R_M = \sqrt{\frac{\alpha}{2} + \sqrt{(\frac{\alpha}{2})^2 - \beta^2}} \tag{5.5}$$

$$R_M = \sqrt{\frac{\alpha}{2}} \tag{5.6}$$

R_M is always positive and R_m is positive for Left Hand Circular Polarization and neg-
ative otherwise. By using the previously stated equations and also some equations related
to the Ellipse, one can calculate the gain of a Right Hand Circular Polarization(*RR*) re-
ceiver antenna and also of a Left Hand one(*RL*). These equations can be seen in 5.7.

$$RR = \frac{R_M - R_m}{2}$$
$$RL = \frac{R_M + R_m}{2} \tag{5.7}$$

5.3 Array Simulation Software Results

Using the software developed it was then possible to, in a constructive way, try to develop
and array of antennas whose Radiation Pattern approximates Isotropy. Initially, it was
decided to place one antenna per lateral faces of the satellite. After some tests made to
understand the interaction between these antennas as a function of the Initial Phase, the
Radiation Pattern presented in figure 5.5 was obtained. The input values that led to this
pattern are presented in figure 5.6. As can be seen, the antennas were placed near a corner
of the cube's faces. This way, a very good pattern was obtained. As predicted, because
no antennas were placed on the top and bottom of the cube, two big nulls appear in the
simulation.

The next logical step was to, using the same configuration, add another sub antenna to
one of the remaining faces of the cube. Therefore, a sub antenna was added to the bottom
face (the one whose vector normal to it is pointing towards -Z). The spatial disposition of
the sub antennas is illustrated in figure 5.7.

After performing a few iterations by varying the Initial Phase of the Electric Field
Phasor, it was decided that this sub antenna should have the following parameters: $X =
0.0155$, $Y = 0.0155$ and $Z = -0.05$, and $\theta = -90^\circ$, $\phi = 0^\circ$ and $\rho_{ini} = 0^\circ$. Very good
results were obtained as can be seen in figure 5.8. The plot on the right clearly shows
that all the volume relative to low and also negative elevation angles has no nulls. The
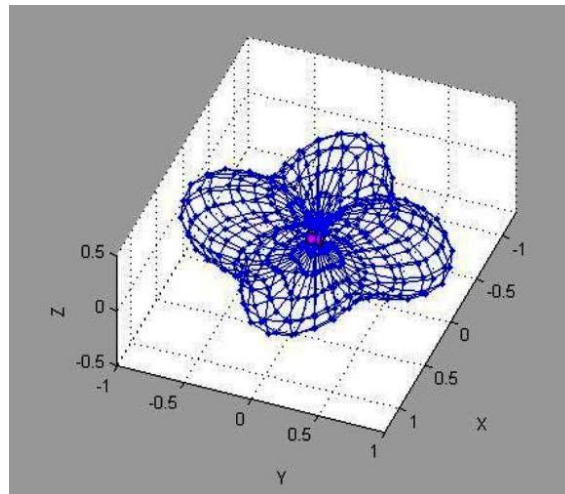lowest value happens for elevations between -50° and -30° and for values of azimuth

Figure 5.5: Radiation Pattern of the four sub antennas- Right Hand Circular Polarization

Figure 5.6: User Input Values relative to the four sub antennas Radiation Pattern

between 40º and 70º. In this volume, the energy received by the array is about half of the maximum value.

It's also important to draw attention to figure 5.9, where the Radiation Pattern of a Left Hand Circularly Polarized receiving antenna is depicted. It's evident that the amount of energy received by the simulated antenna array using this kind of Polarization is much lower, when compared to a Right Hand one.

Finally, there was only one sub antenna missing on the top face of the satellite. Once more, it was put in a corner and the Initial Phase (ρ_{ini}) was varied in order to search for the best results. However, this time the best pattern that one could come up with is presented
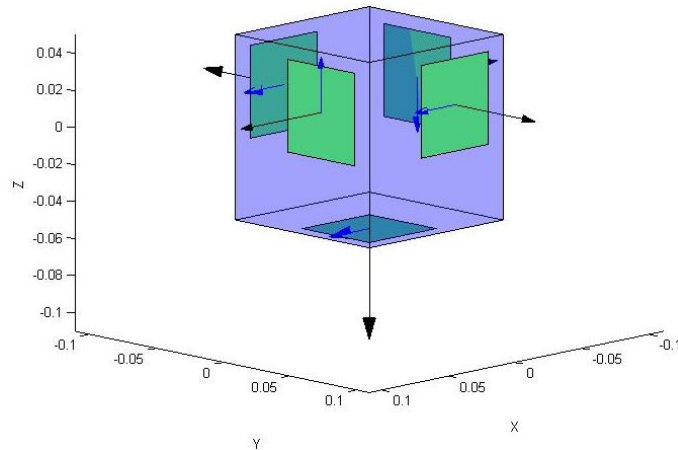
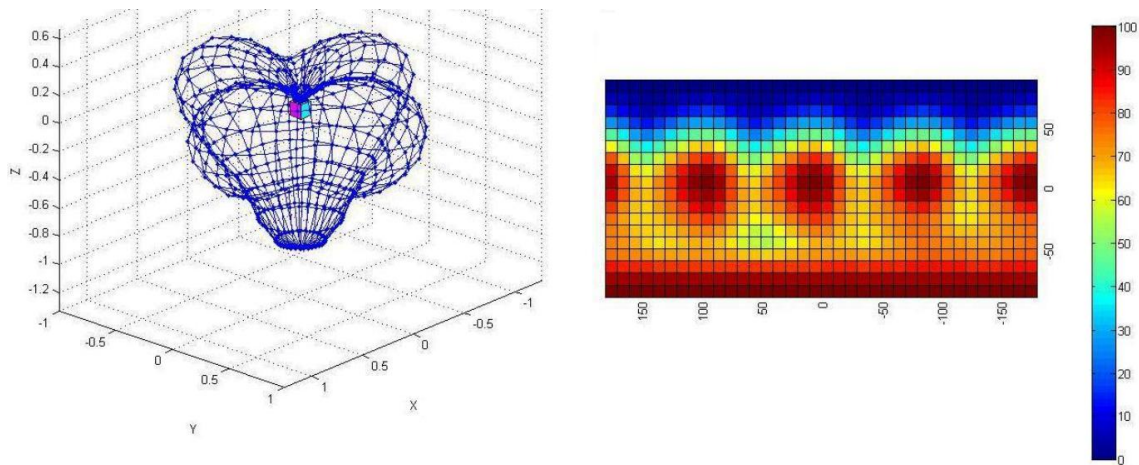Figure 5.7: Spatial disposition of the five sub antennas array

Figure 5.8: Right Hand Circular Polarization Radiation Pattern of the five sub antennas

in figure 5.11. The corresponding input values are stated in 5.10. It can be seen that two nulls exist for elevation angles ranging from 20º to 70º and for azimuth angle values of approximately −130º to −80º and 60º to 130º. This last mentioned null is the biggest one and so the most problematic.

As was already mentioned, in the array simulation software developed, an ideal situation where the Microstrip Patch Antennas only radiate in +/ − 90º relative to the direction normal to its patch was considered. With this in mind, one can reach the conclusion that the problem arises mainly for low to medium elevation angles, because these are the portions of space where the interaction between the antennas truly happens. This way, with the above stated configuration for the array, a destructive interaction between the sub antennas happens in the upper hemisphere. Given the lack of theory found regarding this particular problem, its complexity and the deadlines imposed to this thesis, it was decided
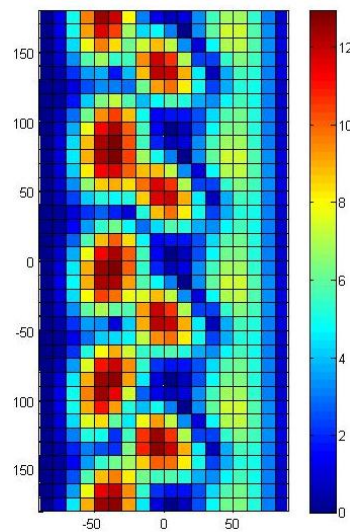
Figure 5.9: Left Hand Circular Polarization Radiation Pattern of the five sub antennas

that an array constituted by 5 sub antennas as was previously presented, would be built. This way, only the lower hemisphere and the lower elevation angles are covered. Still, the built prototype will serve, not only to acquire practical experience, but also to understand if the theory is verified in practice, and if not, what are the issues that should have been taken into consideration. As a final statement, it should be pointed out that the big problem regarding the construction of an Isotropic Radiation Pattern happens in the directions normal to the cube's edges and vertices. This problem can be stated in this way: it's intended that the vectors representing the Initial Phase of the Electric Field Phasor Vector, for each of the sub antennas of the satellite , are such that they assume the same configuration seen from every angle for each vertex of the cube. Also, a solution with more sub antennas can be explored, as long as smaller ones are used.

Some important conclusions can be drawn out from this chapter. In fact, it began with a description of the array simulation software developed in MATLAB. This allowed us to make some important simulations that led to the creation of an array constituted by 5 sub antennas. Although this array will only radiate in some directions and not in all as was initially wanted, its construction will allow us to draw some conclusions about the theory and the software developed. Also, probably the most important conclusion here presented is that the problem regarding the creation of an Isotropic Radiation Pattern with Circular Polarization in a cubic structure is more complex than what was already thought, and it's thought that such pattern cannot be obtained with just one antenna per face.

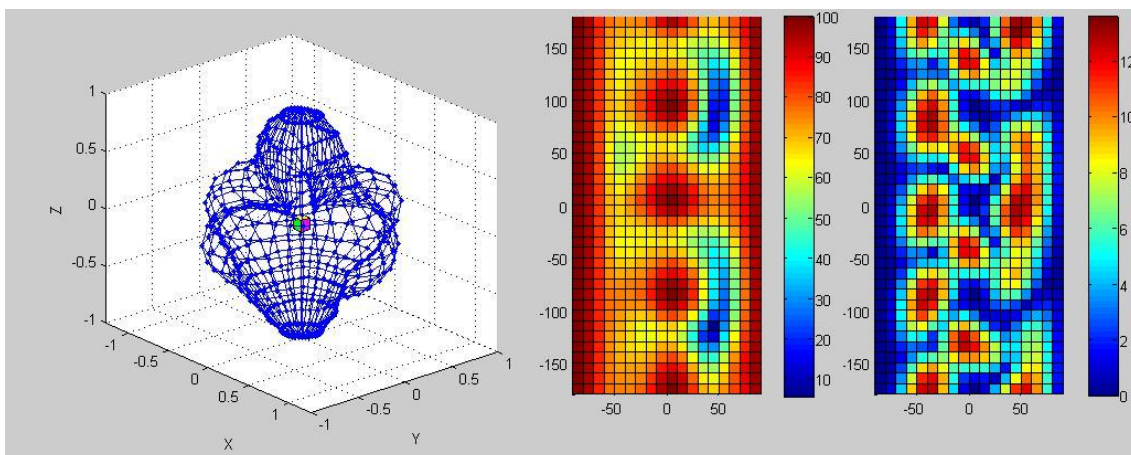Figure 5.10: Input values for the complete six sub antennas array

Figure 5.11: On the left, the Radiation Pattern of 6 antennas array represented in two different graphs and on the right the Left Hand Circular Polarization equivalent graph

Chapter 6

Implementation and Results

In this chapter the built prototype array antenna is presented. The tests performed in the faculty's Anechoic Chamber using this antenna are described. Results concerning this tests are shown and conclusions are drawn out of them.

6.1 The Antenna Array Prototype

With the design of the antenna array described in chapters 4 and 5 it's then possible to finally proceed to the report of its implementation. At this moment it should be pointed out that the Initial Phase difference of each sub antenna was implemented by physically rotating themselves, taking the antennas designed with $\rho_{ini} = 0^{\circ}$ as reference. Although in chapter 4 only one Trimmed Corner Microstrip Patch Antenna simulation was presented, all the other four that constitute the array were also simulated using HFSS. However as the simulations presented similar results, these were considered repetitions of the ones already presented, and therefore excluded from this thesis. Also, one extra antenna identical to the one taken as reference but placed in the middle of a substrate with the same dimensions as a lateral cube's face was simulated. Therefore, six design schematics were sent to the Workshops of the Department of Electrotechnical and Computer Engineering of Porto University. Also the supports for the satellite were made there. The assembled array prototype is shown in figure 6.1. One can notice that the antennas are rotated relatively to one another by observing both the position of the feed (seen as a prominence in the Patch) and of the trimmed corners of each of the three sub antennas visible.

In order to feed the whole array, coaxial cables of a wavelength were used, connected to a dual layer five point star as can be seen in detail in figure 6.2. This star would then connect to the feed cable.

Figure 6.1: The Assembled Prototype

Figure 6.2: The Implemented Feed Scheme for the antenna array

6.2 Prototype Testing and Results

The next step was to test the prototype. For this purpose, the faculty has an Anechoic Chamber for RF testing. The first sub antenna to be tested was the extra one that was developed to work as a Circular Polarized transmitting antenna. Using a Linearly Polarized antenna that already existed at the faculty as an emitter and the Circular Polarized one as a receiver, a conclusion was quickly drawn out. The operating frequency for Circular Polarization was above the intended $1.57542GHz$. In fact, for all the sub antennas, it rounded $1.6GHz$. This can be related to the problems of using FR-4 as a substrate that have been already stated in a previous chapter. Taking into consideration that this is a Prototype, it was decided to solve this problem in the most practical and obvious way, i.e. by increasing the Patch area. However, this could only be done always considering the relation between the Patch area and the cut off area, so that the sub antenna's performance

is maintained. To do so, small cooper wires were soldered around the Patch. This technique proved to be fairly good on solving this problem. This way, it was now possible to proceed to the testing of the array as a whole. An image of the antenna array at the Anechoic Chamber can be seen in 6.3.
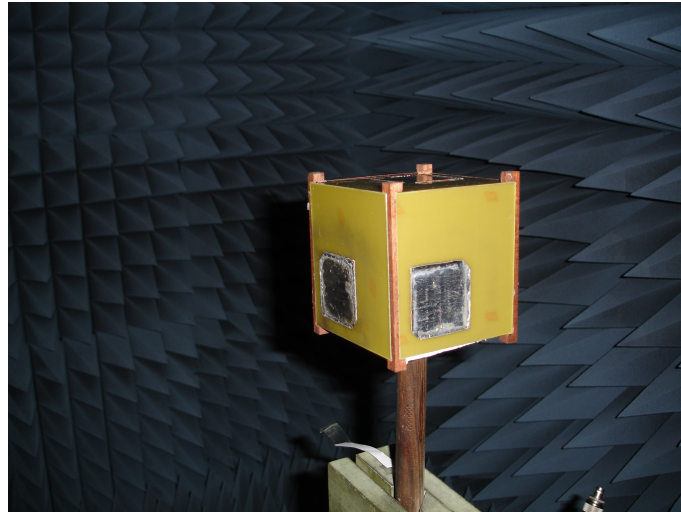
Figure 6.3: Testing the antenna array in the Anechoic chamber

In order to test the array, the extra Right Hand Circular Polarized antenna was used as a transmitter. With the array as a receiver, a couple of pattern cuts were made, in order to be later compared to what had been simulated. The first pattern cut presented in figure 6.4 is for $\theta = 0^o$. On the left a graphic simulated on the array software developed is presented. On the right there is the graphic obtained experimentally. It was expected for the experimental result to have variations of magnitude no bigger than approximately 3.7 dB.
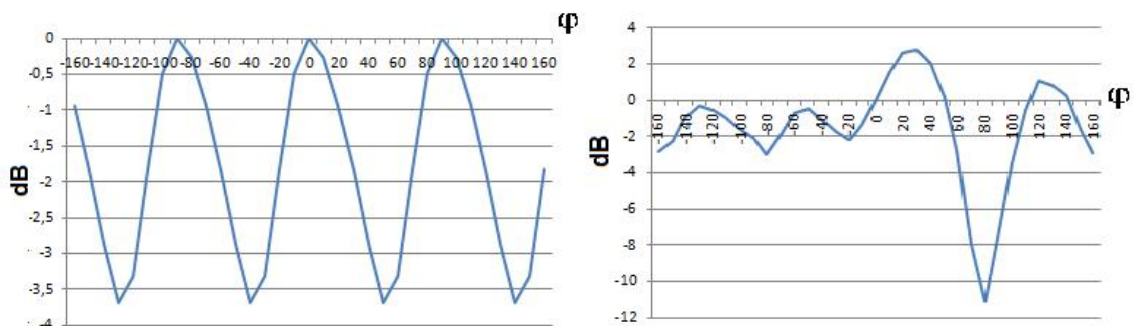
Figure 6.4: $\theta = 0^o$ Pattern Cut.On the left the simulated Pattern cut is represented and on the right one can see the experimentally obtained one

Another pattern cut is presented in figure 6.5. This is referred to $\phi = +/-90^o$. From the results of this cut, one can observe that there are big variations of magnitude.
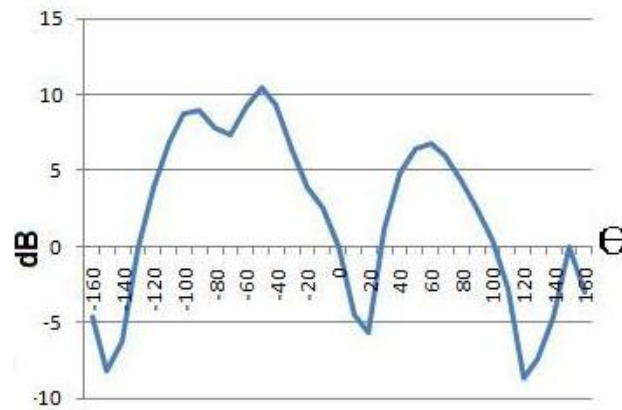
Figure 6.5: $\phi = +/-90^{\circ}$ pattern cut

Because the bottom sub antenna was used as reference(phase and magnitude equal to zero), it's possible to understand from this test, that this sub antenna has a gain inferior to the others, and so, to what was expected. This obviously results in inhomogeneity of the radiated power with consequences for the antenna array Radiation Pattern.

Therefore, it was decided to use this commercial GPS antenna as a transmitter to test the Radiation Pattern of each sub antenna individually. This test led to unexpected results. In fact, some of the sub antennas tested had a Radiation Pattern that didn't match what was expected. Moreover, most of these hit a low magnitude point near the direction normal to the Patch. An example of one of these for the sub antenna located on the face pointing towards $X+$ is presented in contrast to the one obtained from the extra, test transmitter antenna. This can be seen in figure 6.6. From this figure, one can easily observe the contrast.

Figure 6.6: On the left $X+$ antenna Radiation Pattern. On the right the test antenna Radiation Pattern.

In order to better understand if antenna array was working and also to have a general

understanding of its Radiation Pattern, an outdoor receiving GPS test was made. To do so, two 20 dB Gain Line Amplifiers were used. This decision was made after comparing the gain of a commercial GPS antenna to the array one. However the test was unsuccessful as no GPS signals were acquired.
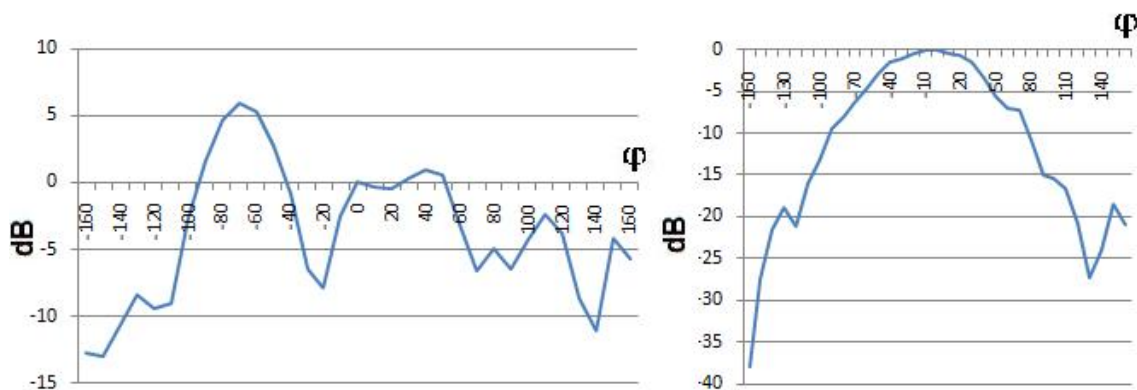
In light of these results, it was decided that the connection scheme that feeds the array should be replaced. This time, a five star pointed star 50Ω microstrip line was used to connect all the five sub antennas to the main feed. Using just one 20 dB Gain Amplifier, the GPS outdoor receiving test was repeated. This time, the results obtained were very good. In fact, the antenna array appeared to receive the GPS signal independently of the direction that was pointed towards the sky. Of course, that when the side of the cube that didn't have a sub antenna was in such direction, the signal received was stronger or satellites with lower altitudes. Next, an analysis of the above stated results will be presented.

6.3   Analysis of the Results

The results obtained from the tests done using the built prototype array antenna revealed some problems. In fact, for both the pattern cuts presented, nulls that were not predicted in the simulation occurred. However it's believed that with a careful, precise, and so more time demanding, testing, better and more accurate results can be obtained. Also, this tests made it possible to understand that the Radiation Pattern of some of the sub antennas that constitute the array was not according to the theory and simulation. This problem obviously affects preponderantly the Radiation Pattern of the antenna array as a whole. Therefore, remaking these sub antennas might be necessary. One other problem detected was related to the use of FR-4 as the substrate. The inaccuracy regarding the Electric Permittivity of this substrate resulted in a antenna operating Frequency Shift. Although the solution proposed in the Literature Review regarding this issue (see figure 3.10) should have been initially considered, the decision to solder small cooper wires in order to raise the Patch area proved to be feasible although time consuming. Other problem that occurred is related to the cables and the connectors. Taking into consideration that the antenna array under development here was just a prototype, it was predicted that there would be the need to replace some of the sub antennas, i.e. that this implementation was an iterative process. As a result, the feeding scheme initially implemented proved to be unsatisfactory. However, its replacement by a new one, led to a very successful outdoor GPS receiving test. This test proved that the built prototype is able to receive GPS signal from various directions.

In this chapter, the prototype and its test results were presented. Unfortunately, the tests proved that there are still some unresolved issues. These issues seem to compromise the theoretically predicted Radiation Pattern of the antenna array. However, the outdoor GPS receiving test performed, led to very good results, validating the functioning of the built antenna array prototype.

Chapter 7

Conclusion and Future Work

In the following sections, the concluded objectives are presented and future perspectives are established.

7.1 Accomplishments and Work Review

In the introductory chapter of this thesis, the main objectives were outlined. This way, goals were established, being that these guided the efforts that were undertaken during its accomplishment. In fact, throughout this thesis, several steps were taken with the main objective of building a prototype GPS antenna array for the Vorsat, whose Radiation Pattern was near Isotropy. Primarily, relatively to the sub antenna design, an algorithm mostly based on the Transmission Line Model and on the Trimmed Square Patch antenna configuration to create Circular Polarization, was employed to design a Trimmed Square Corners Microstrip Patch Antenna. No Input Impedance estimation was made due to its complex analytical calculation as a consequence of this Patch shape. In consequence a software that employed a Full-Wave method was then used. HFSS simulation proved the analytical method to be an efficient one, and so it was validated. At this point, the Input Impedance was adjusted on a trial and error basis, using the simulation software. The next logical step was to design the antenna array itself. For this purpose, a MATLAB software was developed in order to understand the interaction between the sub antennas that constituted the array. After some simulations were performed, conclusions were drawn out. These were related to the number of sub antennas that were going to take part on the array. Initially it was thought that, and due to the space available on the satellite's faces, 6 sub antennas would be used, i.e. one per face. However, the problem of achieving Isotropy quickly proved to be a much more complex one than what was expected. This way, good results could only be achieved using 5 sub antennas (the four lateral ones plus one at the

bottom), covering the lower hemisphere and low elevation angles. In order to respect the thesis deadlines, and also due to the lack of theory found regarding this particular problem, it was decided to implement an array of 5 sub antennas. This way, the design software that was made during this thesis could still be compared to reality and therefore validated. With the implementation made at the Faculty Workshops it was then time to perform the tests on the prototype. However soon some issues regarding its performance were discovered. In fact, the Circular Polarization resonant frequency was at a higher frequency(around $1.6GHz$) than the desired L1 band center frequency($1.57542GHz$). To solve this problem, it was decided to manually increase the Patch area of all the sub antennas of the array, by soldering small cooper wires around the Patch. Although this problem was solved, another one was discovered regarding the Radiation Pattern of some of the sub antennas. This way, the performed tests sometimes didn't show a good correlation between the Radiation Pattern predicted for the array and the one obtained. However it should be mentioned that with more accurate measurement conditions, and perhaps by re-making the problematic sub antennas this problem can be surpassed. Finally, an outdoor GPS receiving test was made. The results obtained were very good. The antenna array was able o receive the GPS signal independently of the direction that was pointed towards the sky. This way, the design strategy as well as the tools developed and presented in this thesis were validated.

7.2 Future Work

Regarding the future work, there are still some important issues that must be addressed. The first and most prominent one is o perform a full and detailed characterization of the antenna array developed. Because there was a limited time for the development of this project, such characterization is yet to be done. Another upgrade to be done to this array is the miniaturization of the Patch antennas. Although there are a couple of solutions to perform this, the easiest way is probably to use Ceramic Substrates. The integration of the Patch antennas with solar panels is another solution that could be added up o this array. In fact, there is already some research published regarding this matter. Some of this is referred throughout this thesis. Finally another pending issue, is related to Isotropy. In fact, as was already mentioned this proved to be a difficult problem. It's possible to delineate two obvious ways that may lead to a solution of this problem. One is to try to find more literature regarding this issue. The other consists on diminishing Patch antenna's size by employing for example a ceramic substrate or other already mentioned methods, with the purpose of placing more than one antenna per face. It's believed that by doing so a solution might be reached. Of course that there will always be a lower point as it was mentioned in the Literature Review that achieving isotropy is impossible.

In this chapter, conclusions regarding the work developed were made. Also future accomplishments were drawn out.

References

[1] C.A. Balanis. *Antenna Theory: Analysis And Design, 2Nd Ed*. Wiley India Pvt. Ltd., 2007.

[2] J.D. Kraus. *Antennas*. McGraw-Hill series in electrical engineering. McGraw-Hill, 1988.

[3] Department of Physics & Astronomy Univeristy of Hawai'i at Manoa. http://www.phys.hawaii.edu/ anita/new/papers/militaryhandbook/polariza.pdf.

[4] Cristiana Monteiro Silva Ramos. Orbit calculation and re-entry control of vorsat satellite, 2011.

[5] Vorsat. http://paginas.fe.up.pt/ cube/.

[6] III Counselman, C.C. Multipath-rejecting gps antennas. *Proceedings of the IEEE*, 87(1):86 –91, jan 1999.

[7] SSTL. http://www.sst-us.com/shop/satellite-subsystems/gps.

[8] Y. Letestu and A. Sharaiha. Multiband printed quadrifilar helical antenna. *Electronics Letters*, 46(13):885 –886, 24 2010.

[9] S. Gao, K. Clark, M. Unwin, J. Zackrisson, W.A. Shiroma, J.M. Akagi, K. Maynard, P. Garner, L. Boccia, G. Amendola, G. Massa, C. Underwood, M. Brenchley, M. Pointer, and M.N. Sweeting. Antennas for modern small satellites. *Antennas and Propagation Magazine, IEEE*, 51(4):40 –56, aug. 2009.

[10] L. Boccia, G. Amendola, and G.D. Massa. Performance evaluation of shorted annular patch antennas for high-precision gps systems. *Microwaves, Antennas Propagation, IET*, 1(2):465 –471, april 2007.

[11] SPantenna. http://www.radiolab.pl/produkty.php?g=18.

[12] N. Padros, J.I. Ortigosa, J. Baker, M.F. Iskander, and B. Thornberg. Comparative study of high-performance gps receiving antenna designs. *Antennas and Propagation, IEEE Transactions on*, 45(4):698 –706, apr 1997.

[13] D.C. Nascimento, J.A. Mores, R. Schildberg, and J.C. da S Lacava. Low-cost truncated corner microstrip antenna for gps application. In *Antennas and Propagation Society International Symposium 2006, IEEE*, pages 1557 –1560, july 2006.

[14] D. C. Nascimento, R. Schildberg, and J. C. da S. Lacava. New considerations in the design of low-cost probe-fed truncated corner microstrip antennas for gps applications. In *Antennas and Propagation Society International Symposium, 2007 IEEE*, pages 749 –752, june 2007.

[15] D. C. Nascimento, R. Schildberg, and J. C. da S. Lacava. Design of low-cost microstrip antennas for glonass applications. *PIERS Online*, 4(7):767 –770, 2008.

[16] R. Garg, P. Bhartia, I. Bahl, and A. Ittipiboon. *Microstrip Antenna Design Handbook*. Artech House, 2001.

[17] V. R. Anitha and S. Narayana Reddy. Design of an 8x1 square microstrip patch antenna array. *International Journal of Electronic Engineering Research*, 1(1):71–77, 2009.

[18] N. Caillet, S. Pinel, C. Quendo, C. Person, E. Rius, J.-F. Favennec, and J. Laskar. A wideband circularly polarized patch array for v-band low-cost applications. In *Microwave Conference, 2007. APMC 2007. Asia-Pacific*, pages 1 –4, dec. 2007.

[19] M.V.T. Heckler, J.C. da S Lacava, and L. Cividanes. Design of a circularly polarized microstrip array mounted on a cylindrical surface. In *Antennas and Propagation Society International Symposium, 2005 IEEE*, volume 2A, pages 266 – 269 vol. 2A, july 2005.

[20] V. Galindo and K. Green. A near-isotropic circulary polarized antenna for space vehicles. *Antennas and Propagation, IEEE Transactions on*, 13(6):872 – 877, nov 1965.

[21] Exame Informática. http://aeiou.exameinformatica.pt/vorsat-o-satelite-de-palmo-e-meio-video=f997516.

[22] C.A. Balanis. Antenna theory: a review. *Proceedings of the IEEE*, 80(1):7 –23, jan 1992.

[23] J. Kraus. Antennas since hertz and marconi. *Antennas and Propagation, IEEE Transactions on*, 33(2):131 – 137, feb 1985.

[24] Nuria Blanco Delgado. *Signal Processing Techniques in Modern Multi-Constellation GNSS Receivers*. PhD thesis, Universidade Técnica de Lisboa-Instituto Superior Técnico, 2010.

[25] QB50. https://www.vki.ac.be/qb50/project.php.

[26] J.M. Tranquilla and S.R. Best. A study of the quadrifilar helix antenna for global positioning system (gps) applications. *Antennas and Propagation, IEEE Transactions on*, 38(10):1545 –1550, oct 1990.

[27] L.I. Basilio, R.L. Chen, J.T. Williams, and D.R. Jackson. A new planar dual-band gps antenna designed for reduced susceptibility to low-angle multipath. *Antennas and Propagation, IEEE Transactions on*, 55(8):2358 –2366, aug. 2007.

[28] Erik O. Hammerstad. Equations for microstrip circuit design. In *Microwave Conference, 1975. 5th European*, pages 268 –272, sept. 1975.

[29] H. F. Mathis. A short proof that an isotropic antenna is impassible. *Proc. IRE*, 39:979, August 1951.

[30] H. F. Mathis. On isotropic antennas. *Proc. IRE*, 42:1810, December 1954.

[31] M. Tanaka, Y. Suzuki, K. Araki, and R. Suzuki. Microstrip antenna with solar cells for microsatellites. *Electronics Letters*, 31(1):5 –6, jan 1995.

[32] N. Henze, A. Giere, H. Fruchting, and P. Hofmann. Gps patch antenna with photo-voltaic solar cells for vehicular applications. In *Vehicular Technology Conference, 2003. VTC 2003-Fall. 2003 IEEE 58th*, volume 1, pages 50 – 54 Vol.1, oct. 2003.

[33] Wen-Shyang Chen, Chun-Kun Wu, and Kin-Lu Wong. Novel compact circularly polarized square microstrip antenna. *Antennas and Propagation, IEEE Transactions on*, 49(3):340 –342, mar 2001.

[34] Eng Gee Lim. *Circular Polarised Microstrip Antenna Using Segmental Methods*. PhD thesis, University of Northumbria at Newcastle, U.K -Division of Electrical and Electronic Engineering, 2002.

[35] W. Richards, Yuen Lo, and D. Harrison. An improved theory for microstrip antennas and applications. *Antennas and Propagation, IEEE Transactions on*, 29(1):38 – 46, jan 1981.

[36] Y.T. Lo, B. Engst, and R.Q. Lee. Simple design formulas for circularly polarised microstrip antennas. *Microwaves, Antennas and Propagation, IEE Proceedings H*, 135(3):213 – 215, jun 1988.

[37] HFSS. hfss.ansoft.co.kr/ug/board.cgi?id=getstart&action=download&gul=3.

[38] CubeSat Specs. http://helpdesk.units.it/sites/atmocube/documenti%20pubblici/cds_rev11.pdf.